© 2019. Published by The Company of Biologists Ltd | Journal of Cell Science (2019) 132, jcs224998. doi:10.1242/jcs.224998

RESEARCH ARTICLE

Akt and SGK protein kinases are required for efficient feeding by macropinocytosis

Thomas D. Williams*, Sew-Yeu Peak-Chew, Peggy Paschke and Robert R. Kay

ABSTRACT

Macropinocytosis is an actin-driven process of large-scale and non-specific fluid uptake used for feeding by some cancer cells and the macropinocytosis model organism *Dictyostelium discoideum*. In *Dictyostelium*, macropinocytic cups are organized by 'macropinocytic patches' in the plasma membrane. These contain activated Ras, Rac and phospholipid PIP3, and direct actin polymerization to their periphery. We show that a *Dictyostelium* Akt (PkbA) and an SGK (PkbR1) protein kinase act downstream of PIP3 and, together, are nearly essential for fluid uptake. This pathway enables the formation of larger macropinocytic patches and macropinosomes, thereby dramatically increasing fluid uptake. Through phosphoproteomics, we identify a RhoGAP, GacG, as a PkbA and PkbR1 target, and show that it is required for efficient macropinocytosis and expansion of macropinocytic patches. The function of Akt and SGK in cell feeding through control of macropinosome size has implications for cancer cell biology.

KEY WORDS: Macropinocytosis, Akt, SGK, Phosphoinositide 3-kinase, PI3K, Endocytosis, *Dictyostelium*

INTRODUCTION

Macropinocytosis is an ancient process used by cells to take up large amounts of fluid (King and Kay, 2018; Swanson, 2008). Actin-driven protrusions are extended in a cup-shape and then closed to engulf extracellular medium into an internal vesicle (Buckley and King, 2017). Macropinocytosis occurs in a variety of mammalian cell types and clinically important settings, perhaps most notably in certain cancer cells as a way of obtaining nutrients (Bloomfield and Kay, 2016; Commisso et al., 2013; Kim et al., 2018; Palm et al., 2017).

Macropinocytic and phagocytic cups are formed by a ring of protrusive F-actin under the plasma membrane that is distinct from other large F-actin structures, such as pseudopods. Several cellular components involved in the organization of these cups have been identified in mammalian and *Dictyostelium discoideum* cells, the most important of which seem to be Ras, Rac1 and the phospholipid PIP3 [phosphatidylinositol (3,4,5)-trisphosphate in mammalian cells, plasmanylinositol (3,4,5)-trisphosphate in *Dictyostelium* (Clark et al., 2014)] (and, by extension, phosphoinositide 3-kinase, PI3K and PTEN, which regulate PIP3) (Araki et al., 2007; Bar-Sagi and Feramisco, 1986; Fujii et al., 2013; Hoeller et al., 2013; Ridley et al., 1992; Veltman et al., 2016; Yoshida et al., 2009).

MRC Laboratory of Molecular Biology, Cambridge, CB2 0QH, UK.

*Author for correspondence (thomasw@mrc-lmb.cam.ac.uk)

T.D.W., 0000-0002-0479-5678; P.P., 0000-0002-6248-5678

Received 14 September 2018; Accepted 19 December 2018

The proteins organizing macropinocytic cups are better known as members of both the growth factor signalling cascade and as oncogenes or tumour suppressors. Growth factors signal through receptor tyrosine kinases (RTKs), which recruit PI3Ks to the plasma membrane and activate downstream effectors such as Ras (Hu et al., 1992; Margolis and Skolnik, 1994). Active Ras, in turn, interacts with class 1 PI3Ks through their Ras-binding domain and activates them to produce PIP3, an interaction that is critical for the growth of certain tumours (Castellano et al., 2013; Gupta et al., 2007). PI3K activation leading to macropinocytosis can also occur independently of Ras (Palm et al., 2017). Activating mutations in the RTK/Ras signalling pathway occur in nearly half of cancers, and activating mutations of the PI3K pathway, mostly PI3Ks and PTEN, in a third, although these groupings include proteins not involved in macropinocytosis (Kandoth et al., 2013; Sanchez-Vega et al., 2018). Ras proteins are especially frequently mutated with, strikingly, ∼95% of pancreatic cancers driven by K-Ras (Fernandez-Medarde and Santos, 2011; Kandoth et al., 2013; Prior et al., 2012; Waddell et al., 2015). Furthermore, loss of the RasGAP NF1 leads to increased Ras activation and tumour development (Bollag et al., 1996; Gutmann et al., 2017).

Macropinocytosis in *Dictyostelium* is highly analogous to macropinocytosis in mammalian cells; however, the situation is simplified as growth factor signalling and RTKs are not present. In *Dictyostelium*, macropinocytosis is used for nutrient acquisition and accounts for the vast majority of fluid uptake, making accurate quantification simple (Hacker et al., 1997; Williams and Kay, 2018a). Additionally, both forward and reverse genetic approaches can be employed (Bloomfield et al., 2015; Paschke et al., 2018).

The *Dictyostelium* macropinocytic cup is formed around a template 'macropinocytic patch' composed of activated Ras and Rac, PIP3 and F-actin, with a rim of the Arp2/3 activators SCAR/WAVE and WASP (Hoeller et al., 2013; Veltman et al., 2016). Other known components are Coronin, the myosin-I proteins and certain formins (Brzeska et al., 2016; Hacker et al., 1997; Junemann et al., 2016). The PIP3-phosphatase PTEN is excluded from the macropinocytic patch, but is present on the rest of the plasma membrane (Hoeller et al., 2013; Iijima and Devreotes, 2002).

PIP3 is vital for efficient macropinocytosis in both amoebae and mammalian cells (Araki et al., 1996; Hoeller et al., 2013; Williams and Kay, 2018b). PIP3 acts by recruiting PIP3-binding proteins to the plasma membrane, often through a PH domain. A considerable number of these proteins exist but which are important for micropinocytosis, and what function they carry out, is not known (Park et al., 2008; Zhang et al., 2010). The Akt protein kinases are oncoproteins that are major downstream effectors of PIP3 in growth factor signalling and mammalian target of rapamycin complex 1 (mTORC1) activation (Dibble and Cantley, 2015; Staal et al., 1977). We examine the role for Akt protein in *Dictyostelium* macropinocytosis.

Journal of Cell Science (2019) 132, jcs224998. doi:10.1242/jcs.224998

Dictyostelium has a single Akt protein, PkbA, with a PIP3-binding PH domain that recruits it to the plasma membrane (Meili et al., 1999; Tanaka et al., 1999). PkbA phosphorylates target proteins at the Akt consensus sequence (RxRxxS/T) (Alessi et al., 1996; Kamimura et al., 2008; Liao et al., 2010). In addition, there is a variant kinase, PkbR1, which was first described as an Akt kinase and is commonly referred to as one, but is more similar to the highly related SGK kinases (Goldberg et al., 2006). PkbR1 is constitutively targeted to the plasma membrane by lipid modification, phosphorylates an overlapping set of target proteins with PkbA and is activated in the same PIP3-dependent manner by TORC2 and phosphoinositide-dependent kinase-1 (PDK1, also known as PDPK1 in mammals) proteins, similar to other SGK kinases (Alessi et al., 1996, 1997; Jacinto et al., 2006; Kamimura and Devreotes, 2010; Kamimura et al., 2008; Kobayashi and Cohen, 1999; Liao et al., 2010; Meili et al., 2000; Murray et al., 2005; Sarbassov et al., 2005; Stephens et al., 1998; Stokoe et al., 1997).

We show here that PkbA and PkbR1, and their activating protein kinases, are required for efficient macropinocytosis. They act downstream of PIP3 to increase macropinosome size, and hence fluid uptake, by increasing the macropinocytic patch size. We identify some of their targets by phosphoproteomics, including the RhoGAP GacG, which is essential for efficient macropinocytosis and without which cells also have reduced macropinosome and macropinocytic patch size.

RESULTS

PkbA and PkbR1 are together required for efficient fluid uptake by macropinocytosis

Fluid uptake by a *Dictyostelium* mutant lacking all five Ras-activated PI3Ks (denoted PI3K1-5-) is practically abolished in shaking culture (Hoeller et al., 2013). However, some mutant strains have a conditional fluid uptake defect in these conditions, which is not apparent when cells are attached to a surface (Novak and Titus, 1997). Additionally, fluid uptake by poorly macropinocytosing cells can sometimes be increased by growing them in medium supplemented with 10% fetal bovine serum (FBS) (Bloomfield et al., 2015). We therefore re-assessed fluid uptake by surface-attached PI3K mutants by using flow cytometry to measure uptake of fluorescent dextran. Fluid uptake was nearly abolished in double-mutants for PI3K1 and PI3K2 (PI3K1-2-) and other multiple PI3K mutants (Fig. 1A), and this was not improved by supplementing the medium with 10% FBS (Fig. S1A).

The protein kinases PkbA (an Akt kinase) and PkbR1 (an SGK kinase) can be activated downstream of PIP3 so could be effectors of PIP3 during the process of macropinocytosis. In vegetative cells, PkbR1 is present on the whole membrane, including

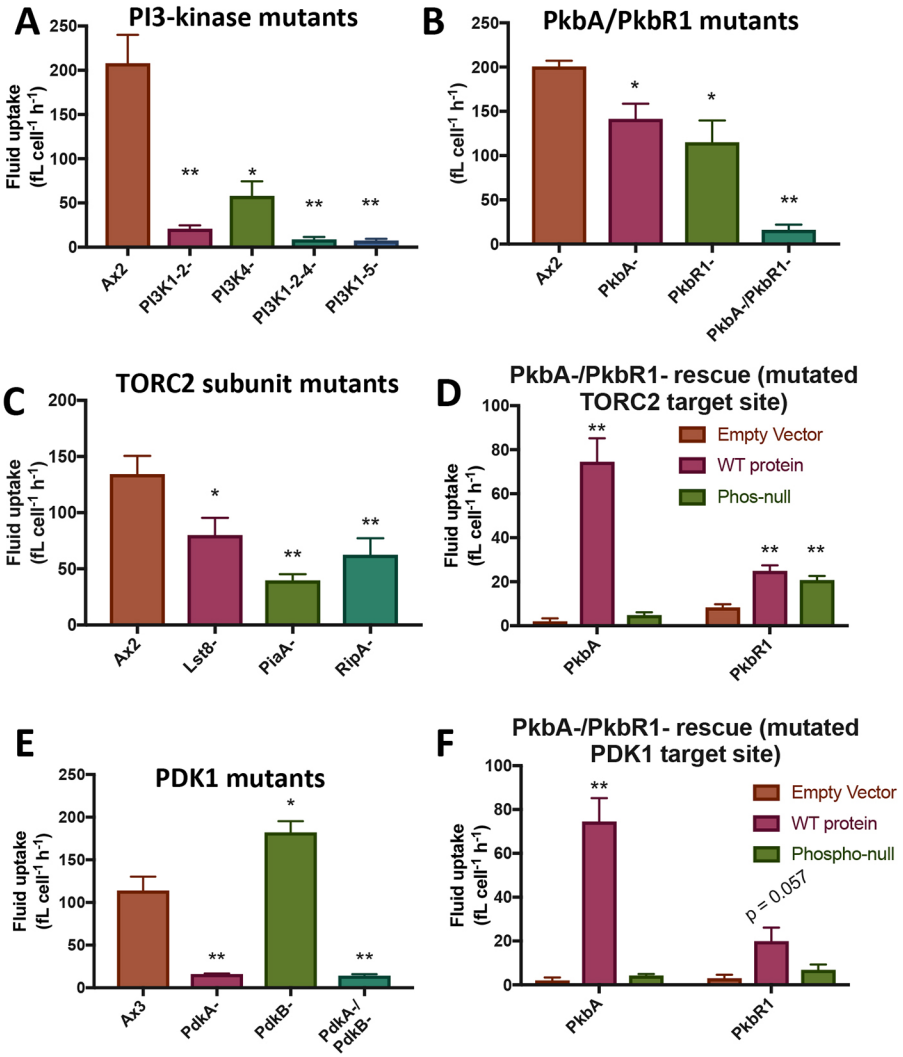

Fig. 1. PkbA/PkbR1 as well as PI3Ks are required for efficient macropinocytic fluid uptake. (A) Fluid uptake is reduced in surface-attached PI3K mutant strains, consistent with previous results in shaking suspension (Hoeller et al., 2013). (B) Fluid uptake is practically abolished in a PkbA-/PkbR1- double mutant, similar to what is seen for the PI3K1-5- strain. (C) Fluid uptake is decreased in knockout mutants of subunits of the TORC2 complex, which activates PkbA/PkbR1 (n=6). (D) Rescue of PkbA-/PkbR1- cells with PkbA was completely abrogated by phospho-null mutation of the TORC2 site, but the equivalent mutation did not affect the rescue by PkbR1. Fluid uptake by PkbA-/PkbR1- cells expressing wild-type (WT) and TORC2-phospho-null (T435A, T470A) versions of PkbA and PkbR1 was measured. The WT versions of the proteins increased fluid uptake, but were not able to rescue fluid uptake to the level of Ax2 cells. (E) Fluid uptake is nearly abolished in the absence of the PDK1 protein PdkA but increased by the absence of the alternative PDK1, PdkB. (F) Rescue of PkbA-/PkbR1- cells with PkbA or PkbR1 was completely abrogated by phospho-null mutation of the PDK1 site. Fluid uptake by PkbA-/PkbR1- cells expressing WT, and PDK1-phospho-null versions of PkbA (T278A) and PkbR1 (T309A) was measured. Cells grown on bacteria were harvested and washed free of bacteria then inoculated into HL5 medium (supplemented with 10% FBS and 20 µg/ml G418 selection for D and F) for at least 24 h, after which TRITC–dextran was added for 1 h. Cells were then washed in ice-cold KK_2 buffer before being detached and analysed by flow cytometry. Graphs show mean±s.e.m., n=3 unless specified. $P\leq0.1$ is specified, *P<0.05, **P<0.01 compared to the parent strain, or strain containing an empty vector control.

Journal of Cell Science (2019) 132, jcs224998. doi:10.1242/jcs.224998

macropinocytic cups (Movie 1). Similar to Akt in mammalian cells, PkbA is recruited specifically to macropinocytic cups, although this occurs most strongly after the cup is initially formed (Movie 2) (Yoshida et al., 2015).

Single and double knockouts of PkbA and PkbR1 (denoted PkbA-, PkbR1- and PkbA-/PkbR1-, respectively) were made in our standard laboratory strain, Ax2 (Ka) (Fig. S1B) using conditions that avoid the need for macropinocytosis-dependent growth (Paschke et al., 2018). Phosphorylation of Akt substrates detected by western blotting was largely unaffected in the single knockouts and in the PI3K1-5- strain but was nearly abolished in the PkbA-/PkbR1- strain (Fig. S1C). This is likely explained by redundancy between PkbA and PkbR1, and PIP3-independent activation of PkbR1 (Kamimura et al., 2008).

Fluid uptake was modestly reduced in the PkbA- and PkbR1- single mutants, in agreement with previous data for PkbA- cells (Rupper et al., 2001). However, it was almost abolished in the double mutant, showing that PkbA and PkbR1 are together essential for effective fluid uptake (Fig. 1B). This also held true in medium supplemented with 10% FBS (Fig. S1D). The PkbA-/PkbR1- mutant phenocopies the PI3K1-5- strain, consistent with PkbA and PkbR1 functioning redundantly as downstream effectors of PIP3. Phenotypes for both strains are henceforth assessed in HL5 medium containing 10% FBS, to guard against possible artefacts due to nutrient starvation.

Since PkbA and PkbR1 are together essential for efficient fluid uptake, we asked whether their activating kinases, TORC2 and PDK1, are also required. TORC2 has four subunits: Tor, PiaA/Rictor, Rip3/Sin1 and Lst8, all of which, excluding Tor, can be knocked out in *Dictyostelium*. These mutants have decreased, but not abolished, activation of PkbA and PkbR1 during chemotaxis (Lee et al., 2005). Fluid uptake was decreased in TORC2 subunit mutants (Fig. 1C), although not to the same extent as in PkbA-/PkbR1- cells, and was largely rescued by supplementation of the medium with 10% FBS (Fig. S1E). As these cells can proliferate in HL5 medium, further assessment of these cells was performed using HL5.

The fluid uptake defect in PkbA-/PkbR1- cells can be substantially, but not entirely, overcome by overexpression of PkbA. However, this rescue was abrogated when the TORC2 site (T435) was mutated to an alanine residue, showing the importance of this phosphorylation (Fig. 1D). In contrast, mutation of the equivalent site in PkbR1, T470, to an alanine residue had no effect on rescue, although the rescue was relatively small. This indicates that PkbR1 activity in the context of macropinocytosis is independent of phosphorylation by TORC2.

Our observation of a fluid uptake defect in the TORC2 subunit mutants is in contrast to what was found in previously published work, where no defect was seen (Rosel et al., 2012). Possible explanations for this difference could be the strain background or previous suppression of the phenotype resulting from prolonged growth in axenic conditions. The fluid uptake defect is, however, consistent with the inhibition of fluid uptake by the Tor inhibitor torin 1 (which inhibits TORC1 and TORC2), while rapamycin (which inhibits TORC1 only) does not inhibit fluid uptake (Rosel et al., 2012; Williams and Kay, 2018b).

Dictyostelium has two PDK1 proteins: PdkA and PdkB. PdkA, but not PdkB, is recruited to PIP3-containing membrane regions, such as macropinosomes, in a PI3K-dependent fashion, although binding to PIP3 has not been shown *in vitro* (Kamimura and Devreotes, 2010; Liao et al., 2010). PdkA could, therefore, be responsible for PIP3-dependent activation of PkbA and PkbR1, like a classical PDK1 protein, with PdkB responsible for PIP3-independent activation of PkbR1 (Alessi et al., 1997; Kamimura et al., 2008; Stokoe et al., 1997). In agreement with this model, fluid uptake by PdkA- mutants was nearly abolished, similar to PI3K1-5- and PkbA-/PkbR1- cells, but was actually increased in PdkB- cells (Fig. 1E). These defects were somewhat ameliorated in medium containing 10% FBS (Fig. S1F). As PdkA- cells can proliferate in non-supplemented HL5 medium, further experiments were performed in this medium.

Mutation of the PDK1 site in PkbA (T278) to an alanine residue resulted in a protein that failed to rescue the fluid uptake defect of PkbA-/PkbR1- cells (Fig. 1F), showing the importance of phosphorylation at this site for macropinocytosis. For PkbR1, in contrast to the seemingly dispensable TORC2 phosphorylation, and consistent with the fluid uptake defect of PdkA- cells, mutation of the PDK1 site (T309) to an alanine residue also prevented rescue (Fig. 1F).

These results show that PkbA and PkbR1 and their activators, TORC2 and PdkA, mediate efficient fluid uptake by macropinocytosis in *Dictyostelium*. PIP3-independent activation of PkbR1 by PdkB seemingly has no function in macropinocytosis. The defect in PkbA-/PkbR1- cells is as severe as in PI3K1-5- cells, and thus could account for their phenotype, though additional PIP3 effectors are not excluded.

PkbA-/PkbR1- cells only have proliferation defects in axenic conditions

Cells utilize macropinocytosis to obtain nutrients for proliferation in liquid medium. As expected from their fluid uptake defect, PkbA-/PkbR1- cells do not proliferate in HL5 medium, either when surface-attached (Fig. 2A) or in shaking suspension (data not shown), consistent with an earlier report using an independently isolated mutant (Meili et al., 2000). Curiously, PkbA- cells have a larger proliferation defect than their fluid uptake defect would suggest. Further investigation revealed that the rate of macropinocytosis decreases in these cells upon prolonged incubation in HL5 medium (Fig. S2A,B), for unknown reasons. Supplementation of the medium with 10% FBS improved the proliferation rates of the PkbA and PkbR1 single mutants, and allowed proliferation of the double mutant (Fig. 2B).

In contrast, cells grown on bacteria obtain nutrients by phagocytosis and have low rates of fluid uptake by macropinocytosis. On bacteria the PkbA/PkbR1 mutants all proliferate at approximately the same rate as the parental Ax2 strain (Fig. 2C), indicating that cellular processes necessary for proliferation are unaffected. As expected, PkbA-/PkbR1- and PI3K1-5- cells were of a comparable size to Ax2 cells when grown on bacteria (Fig. S2C), although they were slightly smaller when in growth medium (Fig. S2D).

Macropinocytosis is strongly upregulated when cells are transferred from bacteria to growth medium, and potentially a failure in this process could underlie the fluid uptake defect in PkbA-/PkbR1- cells. However, we found that PkbA-/PkbR1- cells upregulate macropinocytosis in a similar, although much reduced, way to what is seen in parental Ax2 cells when transferred from growth on bacteria to HL5 medium plus 10% FBS (Fig. 2D).

The normal proliferation of PkbA-/PkbR1- cells on bacteria and our inability to restore normal rates of fluid uptake and proliferation to them in any growth medium tested indicate that they have a specific defect in macropinocytosis, rather than in general cell physiology.

Journal of Cell Science (2019) 132, jcs224998. doi:10.1242/jcs.224998

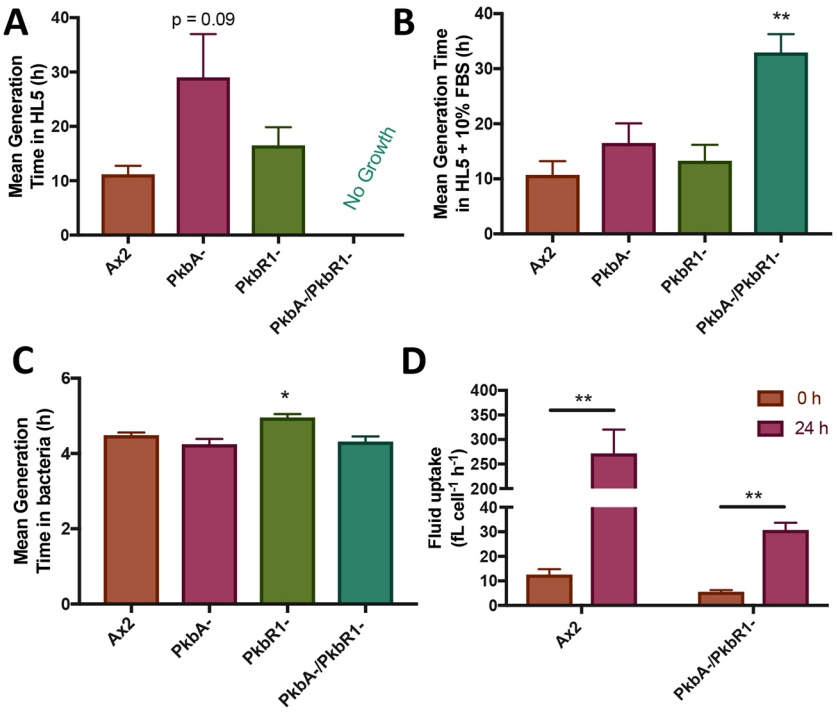

Fig. 2. Proliferation of PkbA/PkbR1 mutants. (A) PkbA-/PkbR1- cells do not proliferate in HL5 medium on a surface, while single-knockout mutants of PkbA have a more severe proliferation defect than expected from their fluid uptake defect. Cells were incubated in HL5 medium for 24 h then distributed into 24-well plates. Proliferation was scored over a week by means of Crystal Violet staining; growth curves were plotted and the mean generation time for each repeat calculated. Similar results were obtained in suspension (data not shown). (B) PkbA-/PkbR1- cells can proliferate, although poorly, when the HL5 medium is supplemented with 10% FBS. Proliferation of single mutants is also improved. Proliferation was determined as in A. (C) Proliferation on bacteria for Ax2 and all the PkbA/PkbR1 mutant strains is similar, apart from a slight growth defect for PkbR1- cells. Cells were harvested from growth on SM bacterial plates and incubated in 20 $OD_{600\ nm}$ *Ka* in KK_2MC at 22°C with shaking at 220 rpm. Cell density was determined at regular intervals using a hemacytometer. (D) PkbA-/PkbR1- cells upregulate macropinocytosis when incubated in HL5 medium plus 10% FBS. Cells were harvested from bacterial plates, washed free of bacteria and incubated in HL5 plus 10% FBS for 0 or 24 h before addition of TRITC–dextran for 1 h. Plates were then washed, and the cells detached for measurement of the fluid uptake by flow cytometry. Graphs show mean±s.e.m., n=3. $P \leq 0.1$ is specified, *$P<0.05$, **$P<0.01$ compared to Ax2.

Macropinocytic patches appear to be normally organized in PkbA-/PkbR1- cells

To investigate the underlying cause of the fluid uptake defect in PkbA-/PkbR1- cells, we examined the organization of their macropinocytic patches. Patches of active Ras and PIP3 were still formed in the mutant (Fig. 3A), and PTEN was excluded from them (Fig. 3B), as expected. F-actin (Fig. 3C) and activated Rac (Fig. 3D) localization, relative to active Ras, was also unperturbed in the mutant. SCAR/WAVE localization was examined using basal patches of active Ras, a surrogate for macropinosomes, as the marker is weak and easily bleached (Veltman et al., 2016) (Fig. 3E). SCAR/WAVE was still enriched at the patch periphery. When this was quantified, no decrease in SCAR/WAVE enrichment at the ring was observed for the PkbA-/PkbR1- cells nor, in this instance, for the PI3K1-5-, contrary to expectations (Veltman et al., 2016).

We could not identify any differences in the organization of macropinocytic patches in the PkbA-/PkbR1- cells, suggesting the reduced fluid uptake is not due to aberrant patch organization.

PkbA and PkbR1 increase the size of macropinocytic patches

We used microscopy to examine the rate at which macropinosomes form and their size. Macropinosomes form at a reduced rate in the PI3K1-5- and PkbA-/PkbR1- strains compared to in the Ax2 strain (Fig. 4A), although this is not statistically significant and cannot account for the entire fluid uptake defect. We ruled out the possibility that these macropinosomes were rapidly recycled to the extracellular medium by using a short uptake time (Fig. S3A).

Instead, we find that PI3K1-5- and PkbA-/PkbR1- mutants form smaller macropinosomes. Macropinosome diameter at internalization was reduced by ∼40% in both cases (Fig. 4B), corresponding to a 3–4-fold decrease in macropinosome volume and thus accounting for a large proportion of the decrease in fluid uptake. A similar reduction in macropinocytic patch size was observed (Fig. 4C), indicating a defect in macropinocytic patch size leads to smaller macropinosomes.

The size of particles that cells can phagocytose correlates with the size of macropinocytic patches formed (Bloomfield et al., 2015; Williams and Kay, 2018b). We measured phagocytosis of various size particles by PkbA-/PkbR1- and PI3K1-5- cells. The PkbA-/PkbR1- and PI3K1-5- mutants were less proficient than Ax2 at uptake of yeast (a comparatively large particle) (Fig. S3B), while phagocytosis of smaller beads was unchanged (Fig. S3C), consistent with the smaller macropinocytic patches made by these mutants.

The TORC2 subunit knockout and PdkA- mutants have similar phenotypes to the PI3K1-5- and PkbA-/PkbR1- cells. Macropinosome formation was reduced, but not to a statistically significant extent, in all the TORC2 subunit mutants, but was significantly reduced for PdkA- cells (Fig. 4D). For all these mutants, macropinosome size was decreased (Fig. 4E). However, although PdkA- mutants had a corresponding decrease in macropinocytic patch size, the TORC2 subunit mutants were largely unaffected in this regard (Fig. 4F). This data is summarized in Fig. 4G.

PI3K1-5- and PkbA-/PkbR1- cells make significantly smaller macropinocytic patches and macropinosomes than their parent, which (due to the cubic relation of linear dimensions and volume) leads to a much larger reduction in macropinosome volume. These results further imply that there is a local positive-feedback loop in which PkbA and PkbR1 increase the activity of upstream macropinocytosis components, such as active Ras, thus enlarging macropinocytic patches.

Identification of PkbA/PkbR1 targets by phosphoproteomics

The postulated feedback loop between upstream macropinocytosis components and PkbA/PkbR1 might operate indirectly and by many different potential routes, but ought to be mediated by targets of both PkbA and PkbR1. We therefore used an unbiased phosphoproteomic screen to identify such targets.

We compared the phosphoproteomes of parental Ax2 cells, PkbA-, PkbR1- and PkbA-/PkbR1- mutants and PkbR1- cells

Journal of Cell Science (2019) 132, jcs224998. doi:10.1242/jcs.224998

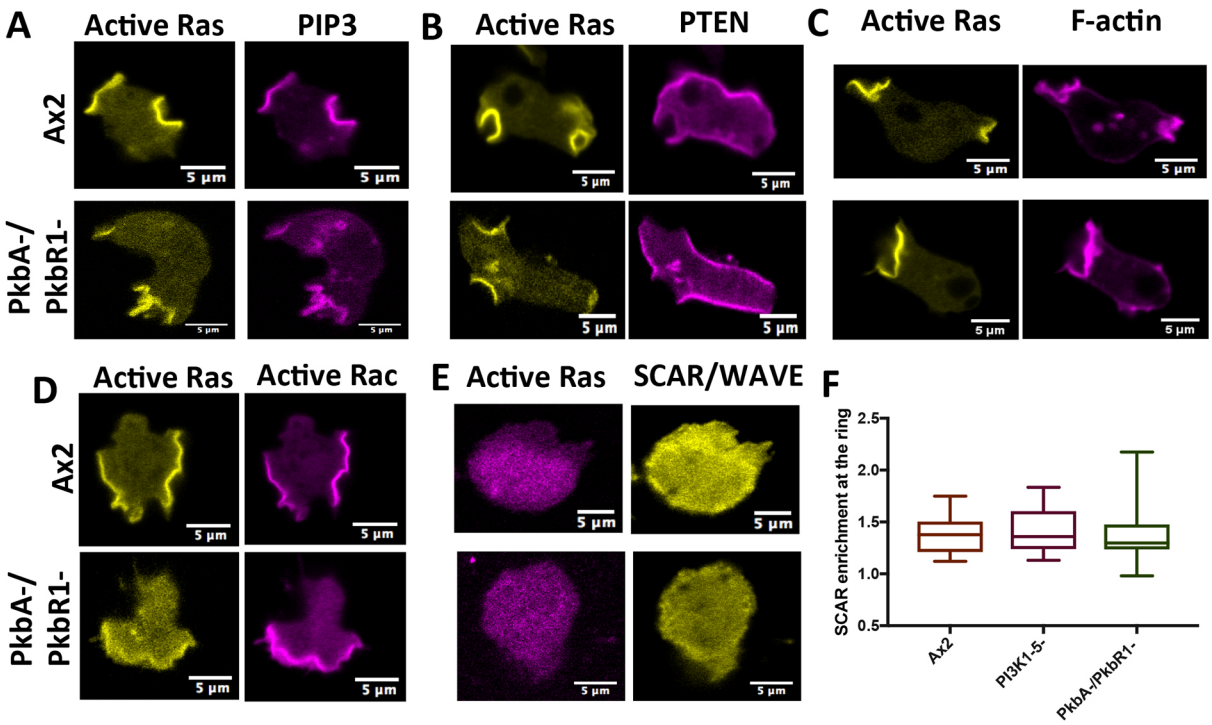

Fig. 3. Macropinocytic patch components are normally localized in PkbA-/PkbR1- cells relative to active Ras. Representative cells show the localization of macropinosome markers relative to active Ras. (A) PIP3 (visualized using PkgE-PH), (B) PTEN (using tagged PTEN), (C) F-actin (using Lifeact), (D) Active Rac (using PakB-CRIB), (E) SCAR/WAVE (using HSPC300). HSPC300–GFP is technically challenging to visualize in macropinocytic patches, as it is faint and easily bleached. Basal patches were used as a surrogate (Veltman et al., 2016). None of the markers were mislocalized relative to active Ras in the PkbA-/PkbR1- mutant. Ax2 and PkbA-/PkbR1- cells were transformed with overexpression vectors containing markers of active Ras and another macropinocytic patch component, then visualized using a Zeiss 700 series microscope. (F) The enrichment of SCAR/WAVE at the circumference of patches was similar between Ax2 and PI3K1-5- or PkbA-/PkbR1- cells, in contrast to previous data showing decreased recruitment in PI3K1-5- cells (Veltman et al., 2016). Cells were imaged on three separate days to obtain images of 32, 28 and 29 basal patches with rings of SCAR/WAVE in the three cell lines, respectively. The SCAR/WAVE ring was defined in a MatLab script that measured the highest fluorescence along a series of orthogonal planes (normals) following its rough outline (Veltman et al., 2016). This was divided by the SCAR/WAVE fluorescence inside the active Ras patch obtained using FIJI software. The graph shows the minimum and maximum values, the box is the 25th to 75th percentile and the middle line shows the median.

treated with LY294002 to inhibit PI3K and hence PkbA. Phosphopeptides were isolated from these cells as described in the Materials and Methods and the relative amounts of each phosphopeptide in each sample were compared by tandem mass tag mass spectrometry over three biological replicates (Table S1). We selected phosphopeptides that were >4-fold decreased in the PkbA-/PkbR1- mutant and >2-fold decreased in the PkbR1- plus LY294002 cells compared to in the Ax2 cells in at least two of the three repeats. A total of 61 peptides from 45 proteins met these criteria.

The kinases likely to be responsible for specific phosphorylations of the filtered set of peptides were predicted using NetPhos 3.1 (Blom et al., 2004). The 16 proteins likely to be phosphorylated by PkbA/PkbR1 (i.e. those with an Akt consensus motif) are shown in Table 1, while the remainder, which are more likely to be phosphorylated by other kinases are in Table S2. Of the potential PkbA/PkbR1 targets, several are predicted to function in signalling, G-protein regulation, intracellular trafficking and digestion (Fig. 5A). Gene Ontology (GO) enrichment analysis of the identified proteins revealed strong enrichment for terms associated with G-protein function, intracellular transport and phosphoinositide binding (Fig. 5B; Table S3) (Ashburner et al., 2000; The Gene Ontology Consortium, 2017). Notably, the terms that contained more than one protein were largely concerned with G-protein regulation. These predicted functions are consistent with proteins involved in cellular feeding by macropinocytosis. Additionally, several of these proteins have previously been identified as PkbA/PkbR1 targets, validating the approach (Charest et al., 2010; Kamimura et al., 2008; Tang et al., 2011).

To assess the extent to which PkbA and PkbR1 phosphorylate overlapping substrates, we identified phosphopeptides that, compared to Ax2, were found >4-fold decreased in one mutant but not the other in at least two of the three repeats. Only a few specific targets were found: KrsB and Kif6 appear to be PkbA-specific targets while DDB_G0278629 and GefS appear to be PkbR1 specific (Table S4).

Since the PkbA/PkbR1-mediated increase in macropinocytic patch size most likely occurs through signalling events, we focused on the targets involved in G-protein function, protein complex scaffold activity and protein kinases. Pats1 mutant (Pats1-) cells have been previously shown not to have an axenic growth defect, so are unlikely to have a macropinocytosis defect and are not analysed further (van Egmond and van Haastert, 2010). A mutant of the scaffold protein (ScaA-) was obtained from the *Dictyostelium* stock centre (Fey et al., 2013; Sawai et al., 2008), while knockout mutants were made of GacG, GacH, GefS and KrsB (denoted GacG-, GacH-, GefS- and KrsB-, respectively) (Fig. S4). We were unable to make a GxcX-knockout mutant.

Fluid uptake of these mutants was measured in HL5 medium (Fig. 5C) and HL5 medium containing 10% FBS (Fig. 5D) and found to only be decreased in ScaA- cells (~50%) and GacG- cells

Journal of Cell Science (2019) 132, jcs224998. doi:10.1242/jcs.224998

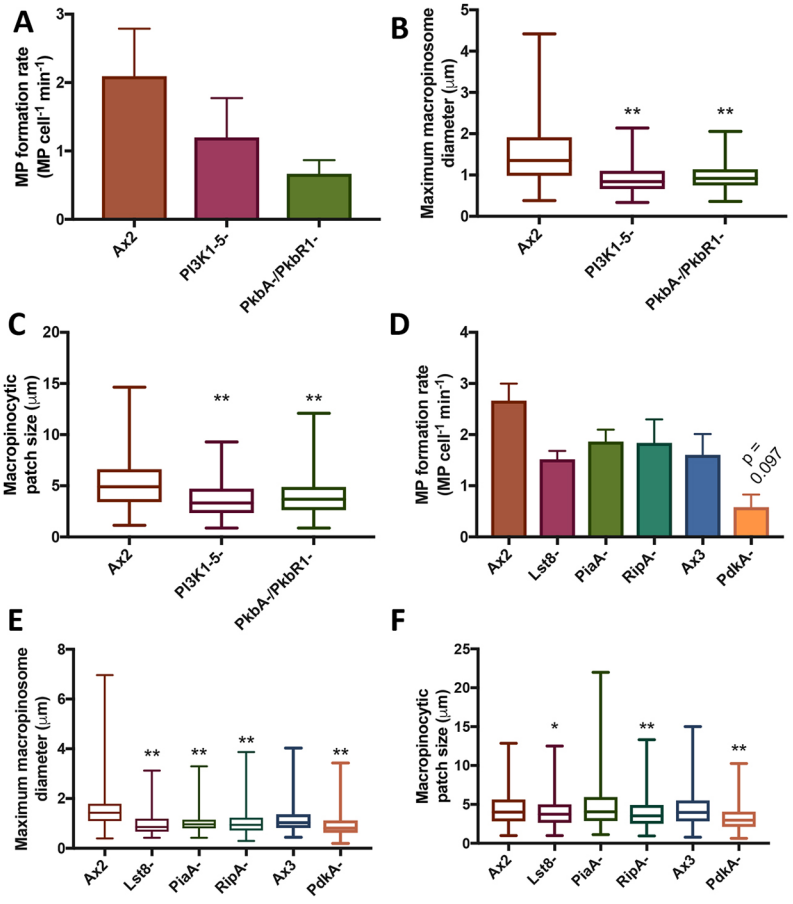

G

Strain	Macropinocytic patch size (%)	Macropinosome "diameter" (%)	Macropinosome radius (%)	Macropinosome volume (%)
Ax2	100 (4.90 μm)	100 (1.35 μm)	100 (0.78 μm)	100 (1.99 μm^3)
PI3K1-5-	68	62	62	24
PkbA-/ PkbR1-	75	68	68	32
Ax2	100 (4.01 μm)	100 (1.43 μm)	100 (0.83 μm)	100 (2.34 μm^3)
Lst8-	93	59	59	21
PiaA-	101	67	67	31
RipA-	88	66	66	29
Ax3	100 (3.96 μm)	100 (1.03 μm)	100 (0.59 μm)	100 (0.89 μm^3)
PdkA-	75	79	79	47

Fig. 4. PkbA/PkbR1 regulate the size of macropinocytic patches. (A) Macropinosome formation was reduced in both PI3K1-5- and PkbA-/PkbR1- strains compared to Ax2, but not by a statistically significant amount. (B) Macropinosome diameter is decreased in PI3K1-5- and PkbA-/PkbR1- cells. This accounts for the majority of the fluid uptake defect. The numbers of macropinosomes analysed were: Ax2, 132; PI3K1-5-, 80; PkbA-/PkbR1-, 75. (C) Macropinocytic patch size is decreased in PI3K1-5- and PkbA-/PkbR1- cells by a similar extent to the macropinosome diameter, indicating this is the reason for the macropinosome size decrease. The numbers of patches analysed were: Ax2, 453; PI3K1-5-, 168; PkbA-/PkbR1-, 330. (D) Macropinosome formation is largely unaffected in TORC2 subunit mutants, but decreased for the PdkA- mutant. (E) Macropinosome size is decreased in the TORC2 subunit and PdkA- mutants. The numbers of macropinosomes analysed were: Ax2, 233; Lst8-, 141; PiaA-, 176; RipA-, 211; Ax3, 141; PdkA-, 202. (F) Macropinocytic patch size is reduced in the PdkA- mutant, but is largely unaffected in the TORC2 subunit mutants. The numbers of patches analysed were: Ax2, 248; Lst8-, 289; PiaA-, 235; RipA-, 232; Ax3, 307; PdkA-, 298. (G) Summary table of the previous figures showing the average values as a percentage of the parental control. The measured diameter tends to halfway between the equator and the poles of the macropinosome (assuming the observed diameters were obtained from random sections of perfectly spherical macropinosomes). The average radius is calculated by multiplying the median observed diameter by tan(30°), and the volume calculated from that. As macropinosomes are often not perfect spheres when they are formed, and sampling at the periphery of macropinosomes is technically challenging, these values are approximate. Cells were harvested from bacteria and inoculated in medium (HL5 medium plus 10% FBS for PI3K1-5- and PkbA-/PkbR1-, HL5 medium for PdkA- and TORC2 mutants, both with appropriate controls) for 24 h, then swapped to SUM before performing the experiments. To measure macropinosome formation, cells were pulsed with FITC–dextran for 1 min, washed and fixed before *Z*-stacks were taken using a Zeiss 710 microscope and the number of macropinosomes per cell counted. Microscopy of macropinocytic patch and macropinosome size were performed on three separate days through random cross-sections of the cells, measured using FIJI software and combined. Macropinosome size was determined by measuring the maximum diameter of the macropinosomes that formed in a mid-section of the cell using an active Ras marker. Macropinocytic patch size was determined by taking tile-scans of cells expressing an active Ras marker focused on the mid-section of the cell and measuring the size of all active Ras patches in the imaged population. Bar graphs show mean±s.e.m.; box plots show the minimum and maximum values, the box is the 25th to 75th percentile and the middle line shows the median; n=3. $P \leq 0.1$ is specified, *P<0.05, **P<0.01 compared to the parent strain.

Journal of Cell Science (2019) 132, jcs224998. doi:10.1242/jcs.224998

Table 1. Candidate PkbA/PkbR1 effector proteins in macropinocytosis

Uniprot ID	Dictybase ID	Phosphosite(s)	Most likely kinase	Predicted function
Q1ZXE9	HipA	S417	Akt	Aids clathrin-actin coupling
Q54G74	DDB_G0290337	S483	Akt	Unknown
Q54QB9	GacG	S461; S469; S480; S730	PKA; GSK3; Akt; PKA	Rho GAP
Q54XY4	ScaA	S225; S228; S232; S359	PKA; CKI; CKII; Akt*	Scaffold protein in PkbA/PkbR1 regulation
Q54YK2	DDB_G0278629	S675; S679	GSK3; Akt	Unknown
Q54ZI7	DynC	S73	Akt	Dynactin subunit
Q552H0	DDB_G0276227	S56	Akt	Rab GTPase
Q55E58	Pats1	T2636	Akt	LRRK family protein kinase
Q55FS2	KrsB	S505	Akt	Protein kinase
Q6S004	Kif6	S1016	Akt	Kinesin
Q75JR6	DDB_G0272206	S1743	Akt	Membrane protein
Q7KWK0	LysA	S847; S851	Akt; Cdc2	Bacterial degradation
Q86HN1	GxcX	S1091	Akt	RhoGEF
Q86IG9	GacH	S355	Akt	RhoGAP
Q86JF2	LvsB	T1193	Akt	Osmotic stress and lysosome organization
Q8SSW7	GefS	S623	Akt	RasGEF

Proteins phosphorylated at an Akt consensus motif (by PkbA/PkbR1) that were less abundant in PkbA-/PkbR1- mutants compared to Ax2 (>4-fold decreased in PkbA-/PkbR1- cells, >2-fold in PkbR1- +LY294002). Cells were harvested from bacterial plates, washed free of bacteria and incubated for 24 h in HL5 medium plus 10% FBS at 22°C with shaking at 220 rpm to allow macropinocytosis upregulation, then washed and resuspended in KK_2MC and treated with 100 µM LY294002 inhibitor or DMSO for 30 min. Proteins were precipitated, labelled with TMT tags, enriched for phosphopeptides and the abundance of each compared between the different mutants using mass spectrometry. The asterisk denotes that this phosphorylation has been shown to be mediated by Akt (Charest et al., 2010), despite the prediction that is slightly more likely to be phosphorylated by PKA than Akt.

(>90%, similar to PI3K1-5- and PkbA-/PkbR1-). Unsurprisingly mutants of KrsB and GefS, which are downstream of only one of the kinases, did not show a fluid uptake defect. That no defect was found for knockouts of the other proteins may be due to redundancy, a compensatory change in macropinosome formation or size, or a lack of involvement. ScaA is part of the Sca1 complex, which has previously been shown to activate TORC2, but is re-localized following phosphorylation by PkbA/PkbR1, limiting PkbA/PkbR1 activation (Charest et al., 2010). We therefore focused on the RhoGAP, GacG.

GacG- mutants have smaller macropinocytic patches

Consistent with the large fluid uptake defect and a potential role downstream of PkbA and PkbR1, GacG- cells are unable to grow in HL5 medium, despite growing relatively normally on bacteria (Fig. 6A; Fig. S5A). They can however grow slowly in HL5 plus 10% FBS (Fig. 6A).

Underpinning the fluid uptake defect are fewer and smaller macropinosomes (Figs 6B,C; Fig. S5B), similar to what is seen for the PI3K1-5- and PkbA-/PkbR1- mutants. Unlike those mutants, however, GacG- cells were much more motile (Fig. S5C–F) (Nichols et al., 2019). The excessive motility made direct measurement of macropinocytic patch size difficult because the same markers are recruited to pseudopods, albeit more faintly, making it difficult to distinguish the two under the conditions used. As a proxy, we instead assessed yeast uptake, finding that this was reduced in GacG- cells to a similar extent to in PI3K1-5- and PkbA-/PkbR1- cells (Fig. 6D; Fig. S3B). Although there was a slight decrease in phagocytosis of smaller particles, this was not significant (Fig. S5G), indicating GacG- cells are less able to phagocytose larger particles. This suggests that GacG- cells, like PI3K1-5- and PkbA-/PkbR1- cells, are defective at making large macropinocytic patches. While overexpression of untagged GacG could rescue the GacG- fluid uptake defect, albeit poorly (Fig. S5H), GacG tagged N- or C-terminally with GFP failed to rescue the fluid uptake defect, preventing a meaningful analysis of GacG localization.

As GacG is predicted to be a RhoGAP, it is likely to function by inactivating a Rho protein. The principal Rho protein involved in macropinocytosis is Rac1, which must be inactivated for macropinosome internalization in mammalian cells and likely also in *Dictyostelium* (Dumontier et al., 2000; Fujii et al., 2013). However, there was no sign of stalled macropinosomes failing to close in GacG- mutants, as would be expected if GacG acted on Rac1. Additionally, patches of active Rac completely colocalize with active Ras patches in GacG- cells, as in Ax2 cells (Figs 6E and 3D). Taken together, these data indicate that GacG does not act on Rac1.

GacG- cells take up much less fluid than Ax2 cells due to a decrease in macropinosome formation rate and size because of the smaller macropinocytic patches. These phenotypes are very similar to that of the PkbA-/PkbR1- and PI3K1-5- mutants, suggesting that GacG lies in the same molecular pathways as a required downstream effector.

DISCUSSION

In this work we show that, together, the protein kinases PkbA and PkbR1 are nearly essential for fluid uptake in *Dictyostelium*. The defect in fluid uptake by PkbA-/PkbR1- cells is as great as that for cells lacking all Ras-activated PI3Ks. In both mutants, this is largely due to a decrease in macropinosome volume due to a reduction in the size of the macropinocytic patches. As PkbA and PkbR1 act downstream of PIP3, lack of activation of PkbA and PkbR1 could account for the phenotype of the PI3K mutants, although a role for other PIP3-binding proteins is not excluded (Fig. 7).

Macropinocytic cups form spontaneously in the plasma membrane of *Dictyostelium* cells, without the need for receptor stimulation. Therefore, the role of the protein kinases PkbA and PkbR1 in macropinocytosis is unlikely to be in conventional signal transduction to activate macropinocytosis. The evidence presented here shows that a major function of PkbA and PkbR1 following their recruitment/activation at PIP3 patches is to make these cups larger, and so able to engulf more liquid or, in the case of phagocytosis, take up larger particles. This role, in which PkbA and PkbR1 activation leads to a local increase in activated Ras (as indicated by larger macropinocytic patches) and hence their activator, PIP3, suggests that PkbA and PkbR1 are part of a local positive-feedback loop.

Journal of Cell Science (2019) 132, jcs224998. doi:10.1242/jcs.224998

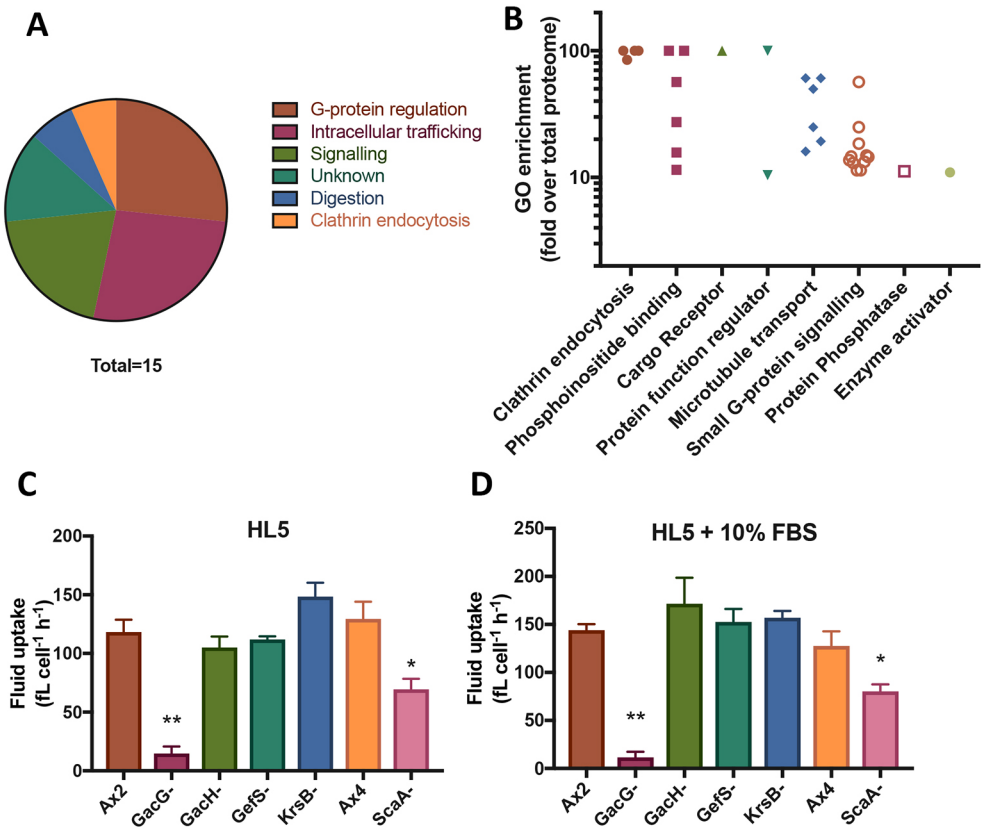

Fig. 5. Fluid uptake by mutants of potential PkbA/PkbR1 targets. (A) Probable functions, taken from Dictybase, of the identified PkbA/PkbR1 target proteins shown in Table 1. Intracellular trafficking, digestion and G-protein regulation are expected for proteins involved in macropinocytosis. (B) The identified proteins are highly enriched for GO terms associated with phosphoinositide binding, G-protein signalling, intracellular microtubule transport and protein regulation, all of which could be expected to have some involvement in macropinocytosis. GO enrichment analysis was performed against the *D. discoideum* reference proteome using the Gene Ontology consortium tools (Ashburner et al., 2000; The Gene Ontology Consortium, 2017). Enriched molecular function terms were identified using the Fisher's exact test. Terms associated with a particular process that are >10-fold enriched are shown (for the exact terms see Table S2). Enrichments over 100-fold are shown as 100-fold enrichments. (C) Fluid uptake by PkbA/PkbR1 target mutants in 1 h after 24 h incubation in HL5 medium after harvesting from bacteria. (D) Fluid uptake by PkbA/PkbR1 target mutants in 1 h after 24 h incubation in HL5 medium plus 10% FBS after harvesting from bacteria. The fluid uptake of the analysed mutants was similar between both media, with defects only seen for the GacG- (a RhoGAP) and ScaA- (a scaffold protein involved in TORC2 activation) mutants. Bar graphs show mean±s.e.m., n=3, *P<0.05, **P<0.01 compared to Ax2; ScaA- is compared to Ax4.

Our search by phosphoproteomics for targets phosphorylated by PkbA and PkbR1 yielded a small list of proteins. Interestingly, several of these are potentially involved in endosome trafficking (microtubule motors, a Rab GTPase and a lysosomal protein were identified), suggesting that PkbA and PkbR1 may have further functions after macropinosome internalization. Focusing instead on proteins potentially involved in a feedback loop to the macropinocytic patch, we showed that mutants of the RhoGAP GacG have extremely poor fluid uptake. As observed for the PkbA-/PkbR1- and PI3K1-5- cells, there was a decrease in macropinosome formation and patch size, suggesting that GacG is an important downstream effector of PkbA and PkbR1 during macropinocytosis.

How GacG affects macropinocytic patch size and formation, and how this is related to the increased motility of the mutant remains to be determined. Although GacG does not appear to inactivate Rac1, other Rho proteins are either present at, or have effects on, the macropinocytic patch (Lee et al., 2003; Rivero et al., 1999; Seastone et al., 1998; Somesh et al., 2006). It is possible that, by switching off one or more of these Rho proteins, a RasGEF could be activated or a RasGAP inhibited, either directly or indirectly, limiting the activation of the Ras-PIP3 pathway (Fig. 7). This would allow cytoskeletal resources to be devoted to forming pseudopods rather than macropinosomes, similar to wild isolates and axenic cells grown on bacteria or entering development, resulting in the observed increase in motility (Fisher et al., 1989; Veltman, 2015; Veltman et al., 2014; Williams and Kay, 2018b). Alternatively, the increase in motility observed in the mutant could be due to an unrelated function of GacG in limiting motility.

In mammalian cells, activating Ras mutations and increased PIP3 production allow macropinocytosis-based feeding, resulting in increased proliferation (Commisso et al., 2013; Kim et al., 2018). Work with *Dictyostelium* implicates several further proteins of the Ras/PI3K pathway in organizing micropinocytosis; apart from Ras itself, the RasGAP NF1, PI3K, PTEN and now an Akt (PkbA) and an SGK (PkbR1) protein kinase, along with their activating kinases, TORC2 and PDK1, are involved. The present work suggests that activating mutations of Akt, and possibly SGK, could drive macropinocytic feeding in mammalian cells, increasing the size of macropinosomes and hence nutrient acquisition. Consistent with this hypothesis, recent studies have shown Akt to be activated at sites of macropinocytosis, while inhibition of macropinocytosis inhibits Akt activation (Chiasson-MacKenzie et al., 2018; Erami et al., 2017; Yoshida et al., 2018). Akt inhibition does not depress macropinosome formation in macrophages, although these studies did not rule out smaller macropinosomes and reduced fluid uptake (Pacitto et al., 2017; Yoshida et al., 2015). Macropinocytic uptake of collagen by hepatic

Journal of Cell Science (2019) 132, jcs224998. doi:10.1242/jcs.224998

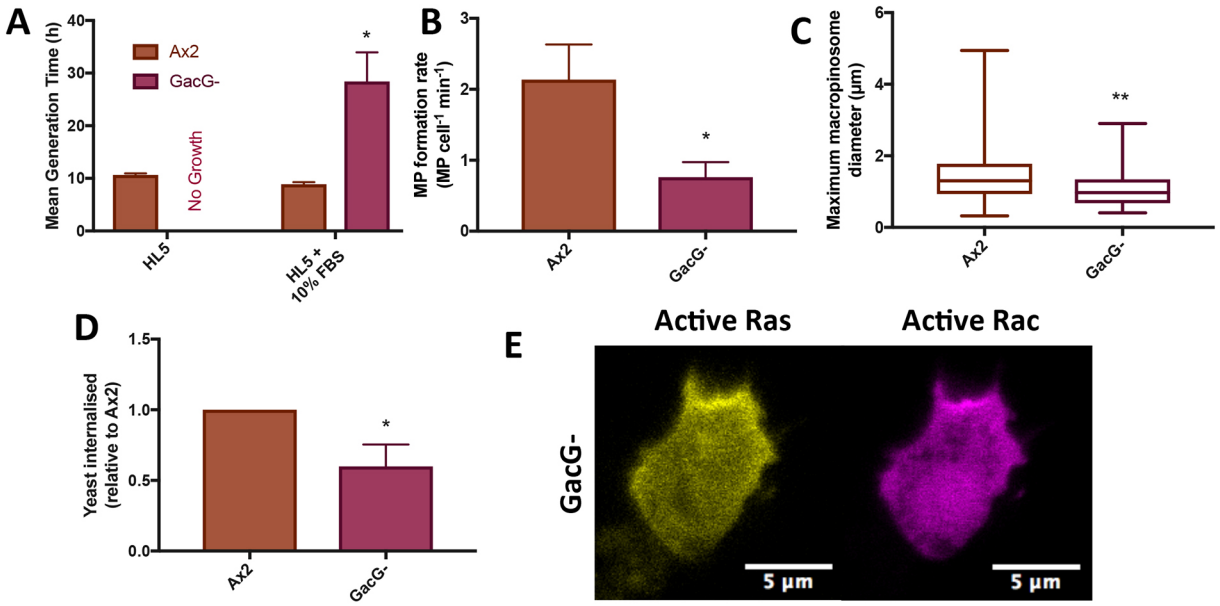

Fig. 6. GacG- cells make fewer and smaller macropinosomes. (A) Consistent with their fluid uptake defect, GacG- cells, like PkbA-/PkbR1- cells, do not proliferate in HL5 medium but do in HL5 plus 10% FBS. Proliferation was measured by using Crystal Violet to stain cells attached to a surface at regular intervals, and the amount of staining quantified. (B) GacG- mutant cells make fewer macropinosomes than Ax2 cells (n=4). Cells that had been incubated in HL5 medium plus 10% FBS for 24 h were pulsed for 1 min with FITC–dextran, fixed using 4% paraformaldehyde and the number of macropinosomes counted using a Zeiss 700 series microscope. (C) GacG- mutant cells make smaller macropinosomes than Ax2 cells. Cells expressing an active Ras marker were filmed on 7 separate days, the diameter of the macropinosomes measured at internalization and the results combined. The numbers of macropinosomes analysed were: Ax2, 254; GacG-, 63. (D) GacG- cells are defective at phagocytosis of fluorescently labelled yeast, like PkbA-/PkbR1- and PI3K1-5- cells, indicating they may have a defect in macropinocytic patch size. Cells were taken from growth on bacteria, washed free of bacteria and incubated with fluorescent yeast for 1 h. Non-internalized yeast were then quenched using Trypan Blue and the fluorescence of internalized yeast was determined using a fluorimeter. (E) Rac1 does not appear to be over-activated, as patches of active Rac that form are still coincident with those of active Ras, similar to what is seen for the Ax2 strain (Fig. 3D). GacG therefore likely inactivates a different Rho protein. Cells were harvested from bacteria and incubated in HL5 medium plus 10% FBS for 24 h before performing the experiments unless otherwise specified. All microscopy was performed on a Zeiss 700 series microscope. Bar graphs show mean±s.e.m., box plots show the minimum and maximum values, the box is the 25th to 75th percentile and the middle line shows the median. n=3 unless specified. *P<0.05, **P<0.01 compared to Ax2.

stellate cells, measured quantitatively by flow cytometry, is reduced by Akt inhibition (Bi et al., 2014). Whether this is due to smaller macropinosomes was not investigated but is a tantalising possibility.

A possible effect on macropinosome size has meaningful implications for the functions of Akt and SGK in tumour growth. The involvement of Akt proteins in the proliferation of cancer cells and tumour development is clear from knockout and inhibitor studies, including in mice with overactivated Ras or PTEN deficiency (Chen et al., 2006; Skeen et al., 2006; Sommer et al., 2013). SGK has been shown to act redundantly with Akt proteins in proliferation of breast cancer cells (Sommer et al., 2013). Decreased proliferation due to decreased Akt activity is usually viewed as being due to decreased mTORC1 activity, but this work suggests a second pathway where Akt and SGK protein kinases increase nutrient acquisition by macropinocytosis, and leads to the prediction that dual inhibition of SGK and Akt kinases would prevent cells feeding by macropinocytosis. A downstream target in mammalian cells similar to GacG would also be a potentially interesting and effective target for a macropinocytosis-specific inhibitor.

MATERIALS AND METHODS

Dictyostelium culture conditions

Dictyostelium discoideum Ax2 (Ka) cells and derivatives were used in this study (see Table S5) and were cultivated on *Klebsiella aerogenes* bacteria on SM plates at 22°C unless otherwise stated. Nutrient media [HL5 (Formedium, UK), HL5 plus 10% FBS and simple uprgulation medium (SUM) (Williams and Kay, 2018b)] were supplemented with dihydrostreptomycin (100 µg/ml), ampicillin (100 µg/ml) and kanamycin (50 µg/ml). Strains were stored frozen in horse serum plus 7.5% DMSO in liquid nitrogen and scraped out using a 16G hypodermic needle (Becton Dickinson) onto *K. aerogenes* and SM agar when needed. Typically, cells were passaged once a week for 4–5 weeks before being refreshed. Except where indicated, we used a standardized set of mutants created in our laboratory strain of Ax2, most of which were made using transformation conditions that did not depend on axenic proliferation, reducing the risk of suppressing mutations.

Cell uptake measurements

All cell uptake measurements were performed as described (Williams and Kay, 2018a,b). Briefly, cells were cultivated on SM agar with *K. aerogenes* bacteria, harvested, washed free of bacteria and inoculated in the indicated nutrient medium to 10^5 cells/ml, with triplicate 50 µl samples in wells of a 96-well plate. This was incubated for 24 h at 22°C before 50 µl of the same medium containing 1 mg/ml TRITC–Dextran (155 kDa, Sigma-Aldrich) was added for 1 h unless otherwise specified. This was then decanted, the plate washed by submersion in ice-cold KK_2 buffer (16.6 mM KH_2PO_4, 3.8 mM K_2HPO_4, pH 6.1) and the cells detached using 100 µl 5 mM sodium azide dissolved in KK_2MC (KK_2 plus 2 mM $MgSO_4$ and 100 µM $CaCl_2$). The fluorescence of each cell in the samples was then measured with an LSR_II flow cytometer (BD Biosciences) and analysed using FlowJo. For the rescue experiments, cells were cultivated in KK_2MC containing two optical density at 600 nm ($OD_{600\ nm}$) units of *Ka* and selection marker in six-well plates, washed three times *in situ* using KK_2MC and inoculated in HL5 medium plus 10% FBS containing selectable marker in a fresh six-well plate. Samples were taken from this plate for up to 3 days after inoculation for fluid uptake measurement.

For measurement of phagocytosis, cells were harvested from bacteria as above. In the case of the 1.5 µm beads (Polysciences) uptake, the cells were diluted into KK_2MC and plated as before, and allowed to settle for ∼30 min.

Journal of Cell Science (2019) 132, jcs224998. doi:10.1242/jcs.224998

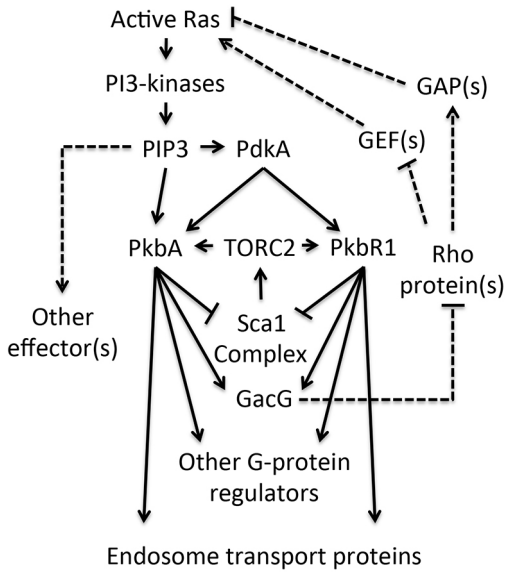

Fig. 7. The Akt activation pathway in *Dictyostelium* macropinocytosis. A patch of active Ras at the plasma membrane recruits and activates class I PI3Ks to synthesize a coincident patch of PIP3 in the plasma membrane. PIP3 recruits PdkA, which, along with the TORC2 complex, activates PkbA (which is also recruited to the PIP3 patch) and PkbR1 (which is constitutively at the plasma membrane). Together, PkbA and PkbR1 phosphorylate effectors, including Sca1 (to dampen further activation of TORC2), proteins involved in endosomal trafficking and G-protein regulators including GacG. GacG is proposed to inactivate an unknown Rho protein(s) which, directly or indirectly, either activates a RasGEF(s), inactivates a RasGAP(s) or both, which would result in the observed restriction of macropinocytic patch size. Proven interactions are shown in bold, while speculative ones shown with dashed lines.

1.5 µm YG beads were washed free of sodium azide and diluted into KK_2MC to 2×10^8 beads/ml. 50 µl of this was added to each well for 20 min, after which cells were washed, detached and internalized fluorescence measured as above and analysed as described previously (Sattler et al., 2013). For yeast uptake, the resuspended cells were placed into 5 ml conical flasks at 5×10^6 cells/ml and shaken for ∼30 min before addition of 10^7 sonicated TRITC-conjugated yeast particles/ml. 200 µl samples were taken at 0 and 60 min, mixed with 2 µl 0.4% Trypan Blue (Sigma-Aldrich) by shaking for 3 min to quench the fluorescence of uninternalized yeast, washed twice in KK_2 plus 10 mM EDTA and the fluorescence determined on a Perkin Elmer LS 50 B fluorimeter (excitation at 544 nm, emission at 574 nm, each with a 10 nm slit).

Transformation of *Dictyostelium*

Vectors were made according to standard procedures, propagated using *Escherichia coli* XL10 and isolated using the ZR miniprep classic kit (Zymogen).

Approximately 10^6 *Dictyostelium* cells were harvested from growth zones on bacterial plates into 1 ml H40 buffer, pelleted by centrifugation at max speed (20,000 ***g***) on a benchtop centrifuge for 10 s and resuspended in 100 µl H40 buffer (Paschke et al., 2018). Vector was added to the cells [500 ng overexpression vector (Table S6) and 2 µg linearized knockout vector (Table S7)] and they were chilled on ice with 2 mm electroporation cuvettes (SLS). The cells were transferred to the 2 mm cuvettes then subject to square wave electroporation in a Bio-Rad GenePulser Xcell (2×350 V for 8 ms, with a 1 s gap) and added to 2 ml KK_2MC plus 2 $OD_{600\ nm}$ *K. aerogenes* in a 3.5 cm dish to recover for 5 h.

After recovery, for cells transformed with an overexpression vector, the appropriate selection antibiotic (10 µg/ml G418, although this was doubled when working with the PkbA-/PkbR1- cells due to poor marker expression, and 100 µg/ml hygromycin) was added to the dish and the dish swirled to ensure an even distribution. In the case of knockout transformations, two 50 ml falcon tubes containing 30 ml KK_2MC plus 2 $OD_{600\ nm}$ *K. aerogenes* and selection antibiotic were prepared, and the dish split between the two tubes (200 µl and 1.8 ml). These were vortexed to mix and 150 µl put into each well of two 96-well plates per tube, and incubated at 22°C. Transformants were typically obtained after 4 days (overexpression) and 6–8 days (knockout).

Screening for mutants

Confluent wells of cells resistant to drug were obtained. To screen these, the medium in the well was pipetted up and down to resuspend the cells and 2 µl from the well was added to 20 µl lysis buffer with 20 µg/ml freshly added proteinase K in a 0.2 ml PCR tube (Paschke et al., 2018). The tube was vortexed to mix, then the proteinase K was inactivated by heating to 95°C for 1 min. 2 µl of DNA was added to a 25 µl PCR reaction to screen for sequence from the resistance cassette to outside the construct, giving a product that could only derive from a mutant (primer sequences are shown in Table S8).

Once wells containing mutants were identified, these were plated clonally onto SM plates with *K. aerogenes* and individual colonies were screened (colony appearance usually took 4 days), with DNA this time being prepared using a g-DNA miniprep kit (Zymogen).

To make double mutants, the resistance cassette in a single mutant strain was removed by Cre-Lox recombination: 500 ng of pDM1489 (Paschke et al., 2018) was transformed into cells, selected for, and then plated out on SM plates with *K. aerogenes* to remove the selective pressure. Clonal populations that had lost both resistance markers were identified; sometimes this took more than one passage of cells on bacteria.

Microscopy

Macropinosome formation rate

Cells were harvested from bacterial plates, washed free of bacteria and incubated in 2 ml of the indicated medium for 24 h at 10^5 cells per well on a six-well plate. The medium was removed, the cells resuspended in 1 ml SUM and transferred to a two-well microscope slide (Nunc) and allowed to settle for ∼1 h. The medium was removed and 0.5 ml SUM containing 2 mg/ml FITC–dextran (70 kDa, Sigma-Aldrich) was added for 1 min, removed and the cells washed twice with KK_2MC, fixed using 4% paraformaldehyde for 20 min, washed five times with PBS (pH 5) and stored at 4°C. *Z*-stacks with 0.1 µm steps were taken using a Zeiss 700 series microscope and the number of dextran-positive vesicles counted manually using FIJI software.

Live-cell microscopy

Cells were transformed with overexpression vectors as above (Table S6). Transformants were washed free of bacteria, and 10^5 cells were incubated in 2 ml medium for 24 h in a six-well plate at 22°C. The medium was removed and replaced with SUM, and the cells transferred to two-well microscope slides for ∼30 min before imaging using a Zeiss 700 series microscope. Movies were typically taken for 5 min with 1 frame per sec. The active Ras marker Raf1-RBD (Hoeller et al., 2013) was used to observe macropinosomes and macropinocytic patches unless otherwise specified. When measuring macropinosome diameters, random cross-sections of cells were used, meaning any individual diameter measured using this technique could be at any section through the macropinosome, but in the aggregate the average tends to halfway between the equator and the poles.

Motility assay

Cells were cultivated on SM agar plates in co-culture with *K. aerogenes* bacteria. At 24 h before the assay, cells were transferred into 2 ml of either HL5 medium plus 10% FBS or a *K. aerogenes*/KK_2MC suspension ($OD_{600\ nm}$=2) at 2×10^5 cells/ml and plated into six-well plates. After 24 h, cells were washed five times in KK_2MC and resuspended in the same buffer to a final density of 10^5 cells per ml. The cells were seeded in MatTek 35 mm Petri dishes with a 20 mm 1.5 coverglass and allowed to attach for 20 min. The random motility of the amoebae was observed for 30 min, taking frames every 30 s using a Zeiss 700 series microscope equipped with a 10× air objective. Automatic cell tracking was performed as described previously (Susanto et al., 2017).

Determination of mean generation time

To measure proliferation in shaking axenic culture, cells were cultured to logarithmic phase in shaking axenic culture, diluted to 5×10^5 cells/ml in fresh medium and counted approximately every 12 h using a haemocytometer.

To measure axenic proliferation of surface attached cells, cells were prepared as above, then 2×10^4 were plated in 0.5 ml fresh medium in duplicate in multiple 24-well plates that were placed in a 22°C incubator. Approximately every 12 h, the medium was removed from a plate, the wells washed once with buffer and stained with 0.1% Crystal Violet dissolved in 10% ethanol for 20 min. The free Crystal Violet was removed by washing three times with water, after which the Crystal Violet staining the cells was dissolved by addition of 0.9 ml 10% acetic acid for 20 min. The absorbance at 590 nm of the resulting solution was obtained using a Nano Drop 2000 (ThermoFisher Scientific) and the background Crystal Violet staining from a set of wells with no cells was subtracted.

Finally, to measure proliferation with bacteria as the food source, cells were cultivated on SM plates in conjunction with *K. aerogenes*. 10^4 cells/ml from growth zones were seeded in a conical flask containing 5 ml KK_2MC plus *K. aerogenes* (at 20 $OD_{600\ nm}$), and the cell density counted approximately every 4 h during the daytime using a haemocytometer.

Western blots

Cells were harvested from SM plates and washed free of bacteria. 10^6 cells were inoculated into 10 ml HL5 medium plus 10% FBS in a 9 cm tissue culture plate for 24 h. They were then resuspended by pipetting, pelleted by centrifugation at 370 ***g*** for 3 min, the supernatant discarded and washed twice in 50 ml ice-cold KK_2MC buffer. Cells were counted and transferred to a 1.5 ml Eppendorf tube, spun down at max speed (20,000 ***g***) in a benchtop centrifuge for 10 s, the supernatant removed by aspiration, resuspended to 2×10^7 cells/ml in 1× sample buffer (NuPage) containing 2.5% 2-mercaptoethanol and protease and phosphatase inhibitors and incubated for 5 min at 95°C.

10 µl of the cell solutions were run on 4–12% Bis-Tris 10-well gels (Nupage) with See Blue Plus 2 used as a ladder. These were blotted onto immobilon P (Merck) membranes. This was blocked with 2% bovine serum albumin (BSA; ThermoFisher Scientific) in Tris-buffered saline with 0.1% Tween 20 (TBS-T) for 2–3 h, then incubated with primary antibody [against α-tubulin (1:1000, DM1A) and phosphorylated Akt substrates (1:1000, 23C8D2), Cell Signaling Technology] overnight in 5% BSA in TBS-T. Membranes were rinsed twice with TBS-T and washed three times for 10 min before addition of the secondary antibody conjugated to HRP (172-011, BioRad and Ab97051, Abcam; 1:10,000) in 5% BSA for 2–3 h, then washed again. Antibodies were imaged with GE Healthcare detection reagent on a BioRad chemidoc using the chemidoc hi-resolution setting. Blots were stripped using restore PLUS western blot stripping buffer (Thermofisher) as per the manufacturer's instructions before re-probing.

Cell size

Cell size was determined using an Eclipse flow cytometer (Sony iCyt). Cells were harvested from growth on bacteria, and incubated in a 24-well plate for 24 h in either HL5 medium plus 10% FBS (10^5 cells/well) or in KK_2MC buffer plus $2OD_{600\ nm}$ *Ka* (10^4 cells/well). They were then washed once *in situ,* resuspended in KK_2MC and passed through a 70 µm filter (Sysmex CellTrics). Cells were then run on the Eclipse to measure the median diameter of the cell population.

Mass spectrometry

Sample preparation for mass spectrometry

Approximately 1×10^8–2×10^8 vegetative cells for each strain (Ax2, PkbA-, PkbR1-, PkbA-/PkbR1-) were harvested from cultivation on bacterial SM agar plates and washed five times in KK_2MC using a benchtop centrifugation at 280 ***g*** for 3 min. The harvested cells were resuspended to 2×10^6 cells per ml in HL5 medium plus 10% FBS, and incubated in a shaking conical flask at 22°C for 24 h.

The cells were then pelleted in a benchtop centrifuge as before, washed twice in KK_2MC and resuspended to 10^7 cells per ml in KK_2MC. The PkbR1- cells were split between two conical flasks, one of which had LY294002 (Cayman Chemical) added to 100 µM (to prevent PkbA recruitment to macropinosomes and activation) while the rest of the samples all had 0.2% DMSO vehicle added (Ax2+DMSO=sample 1, PkbA-+DMSO=sample 2, PkbR1-+DMSO=sample 3, PkbR1-+LY294002=sample 4, PkbA-/PkbR1-+DMSO=sample 5). The cells were incubated shaking at 180 rpm at 22°C for 30 min, then mixed in a 1:1 ratio with 10% trichloroacetic acid (TCA), and incubated on ice for at least 30 min to lyse the cells and precipitate the protein.

The protein was pelleted in a benchtop centrifuge at 2400 ***g*** for 10 min, then washed twice with 20 ml of ice-cold acetone under the same conditions to remove the TCA. The protein was resuspended in protein solubilization buffer (8 M urea, 20 mM HEPES, pH 8) and the concentration of the samples was measured using a Bradford assay (BioRad), adjusted to 2.5 mg/ml, frozen in dry ice and stored at −80°C.

Enzymatic digestion

Following the isolation of protein, 450 µg of each sample was reduced with 5 mM DTT at 56°C for 30 min then alkylated with 10 mM iodoacetamide in the dark at room temperature for 30 min. They were then digested with mass spectrometry grade Lys-C (Promega) at a protein:Lys-C ratio of 150:1 (w/w) for 4 h at 25°C. Next, the samples were diluted from 8 M to 1.5 M urea using 20 mM HEPES (pH 8.5) and digested at 30°C overnight with trypsin (Promega) at a 75:1 (w/w) protein:trypsin ratio. Digestion was stopped by the addition of trifluoroacetic acid (TFA) to a final concentration of 1%. Any precipitates were removed by centrifugation at 13,000 ***g*** for 15 min. The supernatants were desalted using homemade C18 stage tips containing 3 M Empore extraction disks (Sigma-Aldrich) and 8 mg of poros R3 (Applied Biosystems) resin. Bound peptides were eluted with 30–80% acetonitrile (MeCN) in 0.1% TFA and lyophilized.

TMT peptide labelling

The lyophilized peptides from each sample were resuspended in 75 µl of 3% MeCN. The peptide concentrations were determined via a Pierce Quantitative Colorimetric Peptide assay (ThermoFisher Scientific) according to the manufacturers' instructions, except the absorbance was measured by Nanodrop Spectrophotometers (ThermoFisher Scientific) at 480 nm. 0.8 mg of each TMT 10plex reagent (ThermoFisher Scientific) was reconstituted in 41 µl anhydrous MeCN. The peptides from each of the samples were labelled with a distinct TMT tag in 170 mM triethylammonium bicarbonate for 1 h at room temperature. The labelling reaction was stopped by incubation with 8 µl 5% hydroxylamine for 15 min. The labelled peptides from each repeat were combined into a single sample and partially dried to remove MeCN in a SpeedVac (ThermoFisher Scientific). After this, the sample was desalted as before and the eluted peptides were lyophilized.

Phosphopeptide enrichment

The lyophilized labelled peptides were resuspended in 1.2 ml of 50% MeCN and 2 M lactic acid (loading buffer) in an Eppendorf tube and incubated with 20 mg TiO_2 beads (Titansphere, GL Sciences, Japan) at room temperature for 1 h. For the second round of enrichment, the bead slurry was spun down by centrifugation (1657 ***g*** for 2 min), and the supernatant was transferred to another Eppendorf tube. The supernatant was incubated with 15 mg of TiO_2 beads and the bead slurry was spun down again as before. The beads were transferred to homemade C18 stage tips, washed in the tip twice with the loading buffer and once with 50% MeCN plus 0.1% TFA. Phosphopeptides were eluted sequentially with 50 mM K_2HPO_4 (pH 10) followed by 50 mM K_2HPO_4, 50% MeCN (pH 10) and 50% MeCN plus 0.1% TFA. The eluates were partially dried in a SpeedVac after acidification and were desalted as described above.

Basic pH reverse-phase HPLC fractionation

The enriched phosphopeptides were subject to off-line high-performance liquid chromatography (HPLC) fractionation, using an XBridge BEH130 C18, 5 µm, 2.1 mm×150 mm (Waters) column with an XBridge BEH C18 5 µm Van Guard cartridge, connected to an Ultimate 3000 Nano/Capillary LC System (Dionex). Phosphopeptides were resolubilized in solvent A (5% MeCN, 95% 10 mM ammonium bicarbonate, pH 8) and separated with a gradient of 1–90% solvent B (90% MeCN, 10% 10 mM ammonium bicarbonate, pH 8) over

60 min at a flow rate of 250 µl/min. A total of 58 fractions were collected. They were combined into 20 fractions and lyophilized.

LC MS/MS

The fractionated phosphopeptides were analysed by LC tandem mass spectrometry (MS/MS) using a fully automated Ultimate 3000 RSLC nano System (Thermo Scientific) fitted with a 100 µm×2 cm PepMap100 C18 nano trap column and a 75 µm×25 cm reverse phase C18 nano column (Aclaim PepMap, Thermo Scientific). Lyophilized phosphopeptides were dissolved in solvent A (2% MeCN, 0.1% formic acid) and eluted with a linear gradient from 4 to 50% solvent B (80% MeCN, 0.1% formic acid) over 110 min with a flow rate of 300 nl/min. The outlet of the nano column was directly interfaced via a nanospray ion source to a Q Exactive Plus mass spectrometer (Thermo Scientific). The mass spectrometer was operated in standard data-dependent mode, performing a MS full-scan in the *m*/*z* range of 350–1600, with a resolution of 140,000. This was followed by MS2 acquisitions of the 15 most-intense ions with a resolution of 35,000 and normalized collsion energy (NCE) of 33%. MS target values of 3×10^6 and MS2 target values of 10^5 were used. The isolation window of precursor was set at 1.2 Da and sequenced peptides were excluded for 40 s.

Data analysis

The acquired MS/MS raw files from the analysis above were processed using Proteome Discoverer (version 2.1, ThermoFisher Scientific). MS/MS spectra were searched against the January 2016 *Dictyostelium discoideum* UniProt FASTA database, using the Mascot (version 2.4, Matrix Science) search engine. Cysteine carbamidomethylation was set as a fixed modification, while methionine oxidation, N-terminal acetylation (protein), phosphorylation (STY) and TMT6plex (peptide N-terminus and lysine) were selected as variable modifications. Other parameters were set to default values. The abundance values of TMT reporter ions were normalized to total peptide amount. Two output files were generated; one listing the proteins identified and one for peptides. Only proteins and peptides that were identified with a high confidence [false discovery rate (FDR) of <1%] based on a target decoy approach were included in these results. The peptide table was filtered for phosphopeptides with quantitative values and exported as an Excel file.

Quantification and statistical analysis

Statistical analysis was performed using GraphPad prism software, which was used to generate the presented graphs. When there were more than two samples to compare, one-way ANOVA was performed before any further statistical tests. Unless otherwise specified an unpaired *t*-test was performed (*$P\leq0.05$, **$P\leq0.01$ are marked; *P*-values of ≤0.1 are also indicated but are not considered to have reached significance). Unless otherwise stated, the mean is plotted with the error bars showing the s.e.m.

Acknowledgements

The authors thank the Kay laboratory for their input into this project, particularly Gareth Bloomfield and his exhaustive knowledge of the literature, and the LMB microscopy and flow cytometry facilities for excellent scientific and technical support. We are also very grateful to Douwe Veltman for modifying his membrane finder software, Peter Devreotes for providing the PDK1 mutants and Matthew King of Astra Zeneca for support and patience.

Competing interests

The authors declare no competing or financial interests.

Author contributions

Conceptualization: T.D.W., R.R.K.; Methodology: T.D.W., S.-Y.P.-C., P.P.; Validation: T.D.W.; Formal analysis: T.D.W., S.-Y.P.-C., P.P.; Investigation: T.D.W., S.-Y.P.-C., P.P.; Data curation: S.-Y.P.-C.; Writing - original draft: T.D.W.; Writing - review & editing: T.D.W., S.-Y.P.-C., P.P., R.R.K.; Visualization: T.D.W., P.P.; Supervision: R.R.K.; Project administration: R.R.K.; Funding acquisition: R.R.K.

Funding

We thank the Medical Research Council UK for core funding (U105115237) to R.R.K. and AstraZeneca for Blue Sky funding.

Supplementary information

Supplementary information available online at
http://jcs.biologists.org/lookup/doi/10.1242/jcs.224998.supplemental

References

Alessi, D. R., Caudwell, F. B., Andjelkovic, M., Hemmings, B. A. and Cohen, P. (1996). Molecular basis for the substrate specificity of protein kinase B; comparison with MAPKAP kinase-1 and p70 S6 kinase. *FEBS Lett.* **399**, 333-338.

Alessi, D. R., James, S. R., Downes, C. P., Holmes, A. B., Gaffney, P. R. J., Reese, C. B. and Cohen, P. (1997). Characterization of a 3-phosphoinositide-dependent protein kinase which phosphorylates and activates protein kinase Balpha. *Curr. Biol.* **7**, 261-269.

Araki, N., Johnson, M. T. and Swanson, J. A. (1996). A role for phosphoinositide 3-kinase in the completion of macropinocytosis and phagocytosis by macrophages. *J. Cell Biol.* **135**, 1249-1260.

Araki, N., Egami, Y., Watanabe, Y. and Hatae, T. (2007). Phosphoinositide metabolism during membrane ruffling and macropinosome formation in EGF-stimulated A431 cells. *Exp. Cell Res.* **313**, 1496-1507.

Ashburner, M., Ball, C. A., Blake, J. A., Botstein, D., Butler, H., Cherry, J. M., Davis, A. P., Dolinski, K., Dwight, S. S., Eppig, J. T. et al. (2000). Gene ontology: tool for the unification of biology. The Gene Ontology Consortium. *Nat. Genet.* **25**, 25-29.

Bar-Sagi, D. and Feramisco, J. R. (1986). Induction of membrane ruffling and fluid-phase pinocytosis in quiescent fibroblasts by ras proteins. *Science* **233**, 1061-1068.

Bi, Y., Mukhopadhyay, D., Drinane, M., Ji, B., Li, X., Cao, S. and Shah, V. H. (2014). Endocytosis of collagen by hepatic stellate cells regulates extracellular matrix dynamics. *Am. J. Physiol. Cell Physiol.* **307**, C622-C633.

Blom, N., Sicheritz-Pontén, T., Gupta, R., Gammeltoft, S. and Brunak, S. (2004). Prediction of post-translational glycosylation and phosphorylation of proteins from the amino acid sequence. *Proteomics* **4**, 1633-1649.

Bloomfield, G. and Kay, R. R. (2016). Uses and abuses of macropinocytosis. *J. Cell Sci.* **129**, 2697-2705.

Bloomfield, G., Traynor, D., Sander, S. P., Veltman, D. M., Pachebat, J. A. and Kay, R. R. (2015). Neurofibromin controls macropinocytosis and phagocytosis in *Dictyostelium*. *Elife* **4**, e04940.

Bollag, G., Clapp, D. W., Shih, S., Adler, F., Zhang, Y. Y., Thompson, P., Lange, B. J., Freedman, M. H., McCormick, F., Jacks, T. et al. (1996). Loss of NF1 results in activation of the Ras signaling pathway and leads to aberrant growth in haematopoietic cells. *Nat. Genet.* **12**, 144-148.

Brzeska, H., Koech, H., Pridham, K. J., Korn, E. D. and Titus, M. A. (2016). Selective localization of myosin-I proteins in macropinosomes and actin waves. *Cytoskeleton (Hoboken)* **73**, 68-82.

Buckley, C. M. and King, J. S. (2017). Drinking problems: mechanisms of macropinosome formation and maturation. *FEBS J.* **284**, 3778-3790.

Castellano, E., Sheridan, C., Thin, M. Z., Nye, E., Spencer-Dene, B., Diefenbacher, M. E., Moore, C., Kumar, M. S., Murillo, M. M., Grönroos, E. et al. (2013). Requirement for interaction of PI3-kinase p110alpha with RAS in lung tumor maintenance. *Cancer Cell* **24**, 617-630.

Charest, P. G., Shen, Z., Lakoduk, A., Sasaki, A. T., Briggs, S. P. and Firtel, R. A. (2010). A Ras signaling complex controls the RasC-TORC2 pathway and directed cell migration. *Dev. Cell* **18**, 737-749.

Chen, M.-L., Xu, P. Z., Peng, X. D., Chen, W. S., Guzman, G., Yang, X., Di Cristofano, A., Pandolfi, P. P. and Hay, N. (2006). The deficiency of Akt1 is sufficient to suppress tumor development in Pten+/- mice. *Genes Dev.* **20**, 1569-1574.

Chiasson-MacKenzie, C., Morris, Z. S., Liu, C. H., Bradford, W. B., Koorman, T. and McClatchey, A. I. (2018). Merlin/ERM proteins regulate growth factor-induced macropinocytosis and receptor recycling by organizing the plasma membrane:cytoskeleton interface. *Genes Dev.* **32**, 1201-1214.

Clark, J., Kay, R. R., Kielkowska, A., Niewczas, I., Fets, L., Oxley, D., Stephens, L. R. and Hawkins, P. T. (2014). *Dictyostelium* uses ether-linked inositol phospholipids for intracellular signalling. *EMBO J.* **33**, 2188-2200.

Commisso, C., Davidson, S. M., Soydaner-Azeloglu, R. G., Parker, S. J., Kamphorst, J. J., Hackett, S., Grabocka, E., Nofal, M., Drebin, J. A., Thompson, C. B. et al. (2013). Macropinocytosis of protein is an amino acid supply route in Ras-transformed cells. *Nature* **497**, 633-637.

Dibble, C. C. and Cantley, L. C. (2015). Regulation of mTORC1 by PI3K signaling. *Trends Cell Biol.* **25**, 545-555.

Dumontier, M., Hocht, P., Mintert, U. and Faix, J. (2000). Rac1 GTPases control filopodia formation, cell motility, endocytosis, cytokinesis and development in *Dictyostelium*. *J. Cell Sci.* **113**, 2253-2265.

Erami, Z., Khalil, B. D., Salloum, G., Yao, Y., LoPiccolo, J., Shymanets, A., Nürnberg, B., Bresnick, A. R. and Backer, J. M. (2017). Rac1-stimulated macropinocytosis enhances Gbetagamma activation of PI3Kbeta. *Biochem. J.* **474**, 3903-3914.

Fernandez-Medarde, A. and Santos, E. (2011). Ras in cancer and developmental diseases. *Genes Cancer* **2**, 344-358.

Fey, P., Dodson, R. J., Basu, S. and Chisholm, R. L. (2013). One stop shop for everything *Dictyostelium*: dicty Base and the Dicty Stock Center in 2012. *Methods Mol. Biol.* **983**, 59-92.
Fisher, P. R., Merkl, R. and Gerisch, G. (1989). Quantitative analysis of cell motility and chemotaxis in *Dictyostelium discoideum* by using an image processing system and a novel chemotaxis chamber providing stationary chemical gradients. *J. Cell Biol.* **108**, 973-984.
Fujii, M., Kawai, K., Egami, Y. and Araki, N. (2013). Dissecting the roles of Rac1 activation and *Deactivation* in macropinocytosis using microscopic photo-manipulation. *Sci. Rep.* **3**, 2385.
Goldberg, J. M., Manning, G., Liu, A., Fey, P., Pilcher, K. E., Xu, Y. and Smith, J. L. (2006). The *Dictyostelium* kinome–analysis of the protein kinases from a simple model organism. *PLoS Genet.* **2**, e38.
Gupta, S., Ramjaun, A. R., Haiko, P., Wang, Y., Warne, P. H., Nicke, B., Nye, E., Stamp, G., Alitalo, K. and Downward, J. (2007). Binding of ras to phosphoinositide 3-kinase p110alpha is required for ras-driven tumorigenesis in mice. *Cell* **129**, 957-968.
Gutmann, D. H., Ferner, R. E., Listernick, R. H., Korf, B. R., Wolters, P. L. and Johnson, K. J. (2017). Neurofibromatosis type 1. *Nat. Rev. Dis. Primers* **3**, 17004.
Hacker, U., Albrecht, R. and Maniak, M. (1997). Fluid-phase uptake by macropinocytosis in *Dictyostelium*. *J. Cell Sci.* **110**, 105-112.
Hoeller, O., Bolourani, P., Clark, J., Stephens, L. R., Hawkins, P. T., Weiner, O. D., Weeks, G. and Kay, R. R. (2013). Two distinct functions for PI3-kinases in macropinocytosis. *J. Cell Sci.* **126**, 4296-4307.
Hu, P., Margolis, B., Skolnik, E. Y., Lammers, R., Ullrich, A. and Schlessinger, J. (1992). Interaction of phosphatidylinositol 3-kinase-associated p85 with epidermal growth factor and platelet-derived growth factor receptors. *Mol. Cell Biol.* **12**, 981-990.
Iijima, M. and Devreotes, P. (2002). Tumor suppressor PTEN mediates sensing of chemoattractant gradients. *Cell* **109**, 599-610.
Jacinto, E., Facchinetti, V., Liu, D., Soto, N., Wei, S., Jung, S. Y., Huang, Q., Qin, J. and Su, B. (2006). SIN1/MIP1 maintains rictor-mTOR complex integrity and regulates Akt phosphorylation and substrate specificity. *Cell* **127**, 125-137.
Junemann, A., Filić, V., Winterhoff, M., Nordholz, B., Litschko, C., Schwellenbach, H., Stephan, T., Weber, I. and Faix, J. (2016). A Diaphanous-related formin links Ras signaling directly to actin assembly in macropinocytosis and phagocytosis. *Proc. Natl. Acad. Sci. USA* **113**, E7464-E7473.
Kamimura, Y. and Devreotes, P. N. (2010). Phosphoinositide-dependent protein kinase (PDK) activity regulates phosphatidylinositol 3,4,5-trisphosphate-dependent and -independent protein kinase B activation and chemotaxis. *J. Biol. Chem.* **285**, 7938-7946.
Kamimura, Y., Xiong, Y., Iglesias, P. A., Hoeller, O., Bolourani, P. and Devreotes, P. N. (2008). PIP3-independent activation of TorC2 and PKB at the cell's leading edge mediates chemotaxis. *Curr. Biol.* **18**, 1034-1043.
Kandoth, C., McLellan, M. D., Vandin, F., Ye, K., Niu, B., Lu, C., Xie, M., Zhang, Q., McMichael, J. F., Wyczalkowski, M. A. et al. (2013). Mutational landscape and significance across 12 major cancer types. *Nature* **502**, 333-339.
Kim, S. M., Nguyen, T. T., Ravi, A., Kubiniok, P., Finicle, B. T., Jayashankar, V., Malacrida, L., Hou, J., Robertson, J., Gao, D. et al. (2018). PTEN deficiency and AMPK activation promote nutrient scavenging and anabolism in prostate cancer cells. *Cancer Discov.* **8**, 866-883.
King, J. S. and Kay, R. R. (2018). The origins and evolution of macropinocytosis. *Philos. Trans. R. Soc. Lond. B. Biol. Sci.* **374**, http://doi.org/10.1098/rstb.2018.0158.
Kobayashi, T. and Cohen, P. (1999). Activation of serum- and glucocorticoid-regulated protein kinase by agonists that activate phosphatidylinositide 3-kinase is mediated by 3-phosphoinositide-dependent protein kinase-1 (PDK1) and PDK2. *Biochem. J.* **339**, 319-328.
Lee, E., Seastone, D. J., Harris, E., Cardelli, J. A. and Knecht, D. A. (2003). RacB regulates cytoskeletal function in *Dictyostelium* spp. *Euk. Cell* **2**, 474-485.
Lee, S., Comer, F. I., Sasaki, A., McLeod, I. X., Duong, Y., Okumura, K., Yates, J. R., Parent, C. A. and Firtel, R. A. (2005). TOR complex 2 integrates cell movement during chemotaxis and signal relay in *Dictyostelium*. *Mol. Biol. Cell* **16**, 4572-4583.
Liao, X.-H., Buggey, J. and Kimmel, A. R. (2010). Chemotactic activation of *Dictyostelium* AGC-family kinases AKT and PKBR1 requires separate but coordinated functions of PDK1 and TORC2. *J. Cell Sci.* **123**, 983-992.
Margolis, B. and Skolnik, E. Y. (1994). Activation of Ras by receptor tyrosine kinases. *J. Am. Soc. Nephrol.* **5**, 1288-1299.
Meili, R., Ellsworth, C. and Firtel, R. A. (2000). A novel Akt/PKB-related kinase is essential for morphogenesis in *Dictyostelium*. *Curr. Biol.* **10**, 708-717.
Meili, R., Ellsworth, C., Lee, S., Reddy, T. B. K., Ma, H. and Firtel, R. A. (1999). Chemoattractant-mediated transient activation and membrane localization of Akt/PKB is required for efficient chemotaxis to cAMP in *Dictyostelium*. *EMBO J.* **18**, 2092-2105.
Murray, J. T., Cummings, L. A., Bloomberg, G. B. and Cohen, P. (2005). Identification of different specificity requirements between SGK1 and PKBalpha. *FEBS Lett.* **579**, 991-994.
Nichols, J. M., Paschke, P., Peak-Chew, S., Williams, T. D., Tweedy, L., Skehel, M., Stephens, E., Chubb, J. R. and Kay, R. R. (2019). The atypical MAP kinase ErkB transmits distinct chemotactic signals through a core signalling module. *Dev. Cell* (in press). doi:10.1016/j.devcel.2018.12.001.
Novak, K. D. and Titus, M. A. (1997). Myosin I overexpression impairs cell migration. *J. Cell Biol.* **136**, 633-647.
Pacitto, R., Gaeta, I., Swanson, J. A. and Yoshida, S. (2017). CXCL12-induced macropinocytosis modulates two distinct pathways to activate mTORC1 in macrophages. *J. Leukoc. Biol.* **101**, 683-692.
Palm, W., Araki, J., King, B., DeMatteo, R. G. and Thompson, C. B. (2017). Critical role for PI3-kinase in regulating the use of proteins as an amino acid source. *Proc. Natl. Acad. Sci. USA* **114**, E8628-E8636.
Park, W. S., Heo, W. D., Whalen, J. H., O'Rourke, N. A., Bryan, H. M., Meyer, T. and Teruel, M. N. (2008). Comprehensive identification of PIP3-regulated PH domains from C. elegans to H. sapiens by model prediction and live imaging. *Mol. Cell* **30**, 381-392.
Paschke, P., Knecht, D. A., Silale, A., Traynor, D., Williams, T. D., Thomason, P. A., Insall, R. H., Chubb, J. R., Kay, R. R. and Veltman, D. M. (2018). Rapid and efficient genetic engineering of both wild type and axenic strains of *Dictyostelium discoideum*. *PLoS ONE* **13**, e0196809.
Prior, I. A., Lewis, P. D. and Mattos, C. (2012). A comprehensive survey of Ras mutations in cancer. *Cancer Res.* **72**, 2457-2467.
Ridley, A. J., Paterson, H. F., Johnston, C. L., Diekmann, D. and Hall, A. (1992). The small GTP-binding protein rac regulates growth factor-induced membrane ruffling. *Cell* **70**, 401-410.
Rivero, F., Albrecht, R., Dislich, H., Bracco, E., Graciotti, L., Bozzaro, S. and Noegel, A. A. (1999). RacF1, a novel member of the Rho protein family in *Dictyostelium discoideum*, associates transiently with cell contact areas, macropinosomes, and phagosomes. *Mol. Biol. Cell* **10**, 1205-1219.
Rosel, D., Khurana, T., Majithia, A., Huang, X., Bhandari, R. and Kimmel, A. R. (2012). TOR complex 2 (TORC2) in *Dictyostelium* suppresses phagocytic nutrient capture independently of TORC1-mediated nutrient sensing. *J. Cell Sci.* **125**, 37-48.
Rupper, A., Lee, K., Knecht, D. and Cardelli, J. (2001). Sequential activities of phosphoinositide 3-kinase, PKB/Akt, and Rab7 during macropinosome formation in *Dictyostelium*. *Mol. Biol. Cell* **12**, 2813-2824.
Sanchez-Vega, F., Mina, M., Armenia, J., Chatila, W. K., Luna, A., La, K. C., Dimitriadoy, S., Liu, D. L., Kantheti, H. S., Saghafinia, S. et al. (2018). Oncogenic signaling pathways in the cancer genome atlas. *Cell* **173**, 321-337 e10.
Sarbassov, D. D., Guertin, D. A., Ali, S. M. and Sabatini, D. M. (2005). Phosphorylation and regulation of Akt/PKB by the rictor-mTOR complex. *Science* **307**, 1098-1101.
Sattler, N., Monroy, R. and Soldati, T. (2013). Quantitative analysis of phagocytosis and phagosome maturation. *Methods Mol. Biol.* **983**, 383-402.
Sawai, S., Guan, X. J., Kuspa, A. and Cox, E. C. (2008). High-throughput analysis of spatio-temporal dynamics in *Dictyostelium*. *Genome Biol.* **8**, R144.
Seastone, D. J., Lee, E., Bush, J., Knecht, D. and Cardelli, J. (1998). Overexpression of a novel Rho family GTPase, RacC, induces unusual actin-based structures and positively affects phagocytosis in *Dictyostelium discoideum*. *Mol. Biol. Cell* **9**, 2891-2904.
Skeen, J. E., Bhaskar, P. T., Chen, C.-C., Chen, W. S., Peng, X.-D., Nogueira, V., Hahn-Windgassen, A., Kiyokawa, H. and Hay, N. (2006). Akt deficiency impairs normal cell proliferation and suppresses oncogenesis in a p53-independent and mTORC1-dependent manner. *Cancer Cell* **10**, 269-280.
Somesh, B. P., Vlahou, G., Iijima, M., Insall, R. H., Devreotes, P. and Rivero, F. (2006). RacG regulates morphology, phagocytosis and chemotaxis. *Euk. Cell* **5**, 1648-1663.
Sommer, E. M., Dry, H., Cross, D., Guichard, S., Davies, B. R. and Alessi, D. R. (2013). Elevated SGK1 predicts resistance of breast cancer cells to Akt inhibitors. *Biochem. J.* **452**, 499-508.
Staal, S. P., Hartley, J. W. and Rowe, W. P. (1977). Isolation of transforming murine leukemia viruses from mice with a high incidence of spontaneous lymphoma. *Proc. Natl. Acad. Sci. USA* **74**, 3065-3067.
Stephens, L., Anderson, K., Stokoe, D., Erdjument-Bromage, H., Painter, G. F., Holmes, A. B., Gaffney, P. R., Reese, C. B., McCormick, F., Tempst, P. et al. (1998). Protein kinase B kinases that mediate phosphatidylinositol 3,4,5-trisphosphate-dependent activation of protein kinase B. *Science* **279**, 710-714.
Stokoe, D., Stephens, L. R., Copeland, T., Gaffney, P. R., Reese, C. B., Painter, G. F., Holmes, A. B., McCormick, F. and Hawkins, P. T. (1997). Dual role of phosphatidylinositol-3,4,5-trisphosphate in the activation of protein kinase B. *Science* **277**, 567-570.
Susanto, O., Koh, Y. W. H., Morrice, N., Tumanov, S., Thomason, P. A., Nielson, M., Tweedy, L., Muinonen-Martin, A. J., Kamphorst, J. J., Mackay, G. M. et al. (2017). LPP3 mediates self-generation of chemotactic LPA gradients by melanoma cells. *J. Cell Sci.* **130**, 3455-3466.
Swanson, J. A. (2008). Shaping cups into phagosomes and macropinosomes. *Nat. Rev. Mol. Cell Biol.* **9**, 639-649.
Tanaka, K., Adachi, H., Konishi, H., Iwamatsu, A., Ohkawa, K., Shirai, T., Nagata, S., Kikkawa, U. and Fukui, Y. (1999). Identification of protein kinase B (PKB) as a phosphatidylinositol 3,4,5-trisphosphate binding protein in *Dictyostelium discoideum*. *Biosci. Biotechnol. Biochem.* **63**, 368-372.

Tang, M., Iijima, M., Kamimura, Y., Chen, L., Long, Y. and Devreotes, P. (2011). Disruption of PKB signaling restores polarity to cells lacking tumor suppressor PTEN. *Mol. Biol. Cell* **22**, 437-447.
The Gene Ontology Consortium (2017). Expansion of the Gene Ontology knowledgebase and resources. *Nucleic Acids Res.* **45**, D331-D338.
van Egmond, W. N. and van Haastert, P. J. (2010). Characterization of the Roco protein family in *Dictyostelium discoideum*. *Eukaryot. Cell* **9**, 751-761.
Veltman, D. M. (2015). Drink or drive: competition between macropinocytosis and cell migration. *Biochem. Soc. Trans.* **43**, 129-132.
Veltman, D. M., Lemieux, M. G., Knecht, D. A. and Insall, R. H. (2014). PIP(3)-dependent macropinocytosis is incompatible with chemotaxis. *J. Cell Biol.* **204**, 497-505.
Veltman, D. M., Williams, T. D., Bloomfield, G., Chen, B.-C., Betzig, E., Insall, R. H. and Kay, R. R. (2016). A plasma membrane template for macropinocytic cups. *Elife* **5**, e20085.
Waddell, N., Pajic, M., Patch, A.-M., Chang, D. K., Kassahn, K. S., Bailey, P., Johns, A. L., Miller, D., Nones, K., Quek, K. et al. (2015). Whole genomes redefine the mutational landscape of pancreatic cancer. *Nature* **518**, 495-501.
Williams, T. D. and Kay, R. R. (2018a). High-throughput measurement of *Dictyostelium discoideum* macropinocytosis by flow cytometry. *J. Vis. Exp.* **139**, e58434.
Williams, T. D. and Kay, R. R. (2018b). The physiological regulation of macropinocytosis during *Dictyostelium* growth and development. *J. Cell Sci.* **131**, jcs213736.
Yoshida, S., Hoppe, A. D., Araki, N. and Swanson, J. A. (2009). Sequential signaling in plasma-membrane domains during macropinosome formation in macrophages. *J. Cell Sci.* **122**, 3250-3261.
Yoshida, S., Gaeta, I., Pacitto, R., Krienke, L., Alge, O., Gregorka, B. and Swanson, J. A. (2015). Differential signaling during macropinocytosis in response to M-CSF and PMA in macrophages. *Front. Physiol.* **6**, 8.
Yoshida, S., Pacitto, R., Sesi, C., Kotula, L. and Swanson, J. A. (2018). Dorsal ruffles enhance activation of Akt by growth factors. *J. Cell Sci* **131**, jcs220517.
Zhang, P., Wang, Y., Sesaki, H. and Iijima, M. (2010). Proteomic identification of phosphatidylinositol (3,4,5) triphosphate-binding proteins in *Dictyostelium discoideum*. *Proc. Natl. Acad. Sci. USA* **107**, 11829-11834.

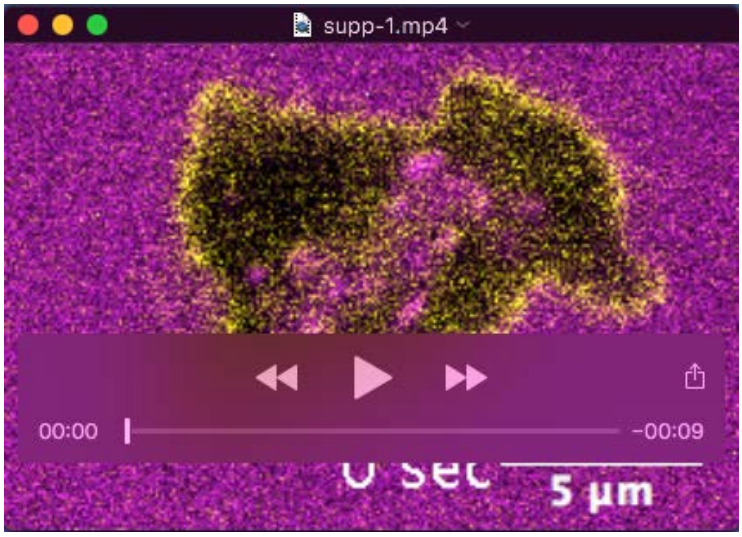

Movie 1: PkbR1-GFP is present on macropinosomes
PkbA-/PkbR1- cell overexpressing PkbR1-GFP (yellow) in TRITC-dextran containing media (magenta). PkbR1-GFP is present all over the cell membrane, including the macropinocytic cup, which is internalised and PkbR1-GFP remains on the endosome for a time after internalisation. Movie was taken at one frame per second on a Zeiss 710 microscope.

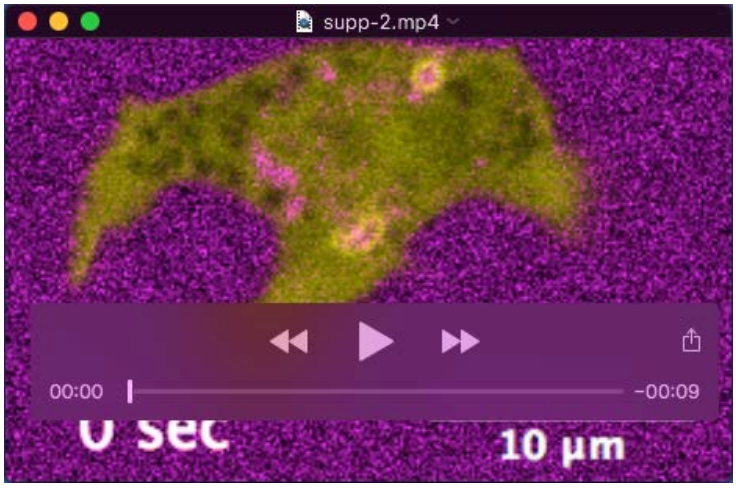

Movie 2: GFP-PkbA labels macropinosomes
PkbA-/PkbR1- cell overexpressing GFP-PkbA (yellow) in TRITC-dextran containing media (magenta). GFP-PkbA is recruited to macropinocytic cups and remains on endosomes for a time after internalisation. Movie was taken at one frame per second on a Zeiss 710 microscope.

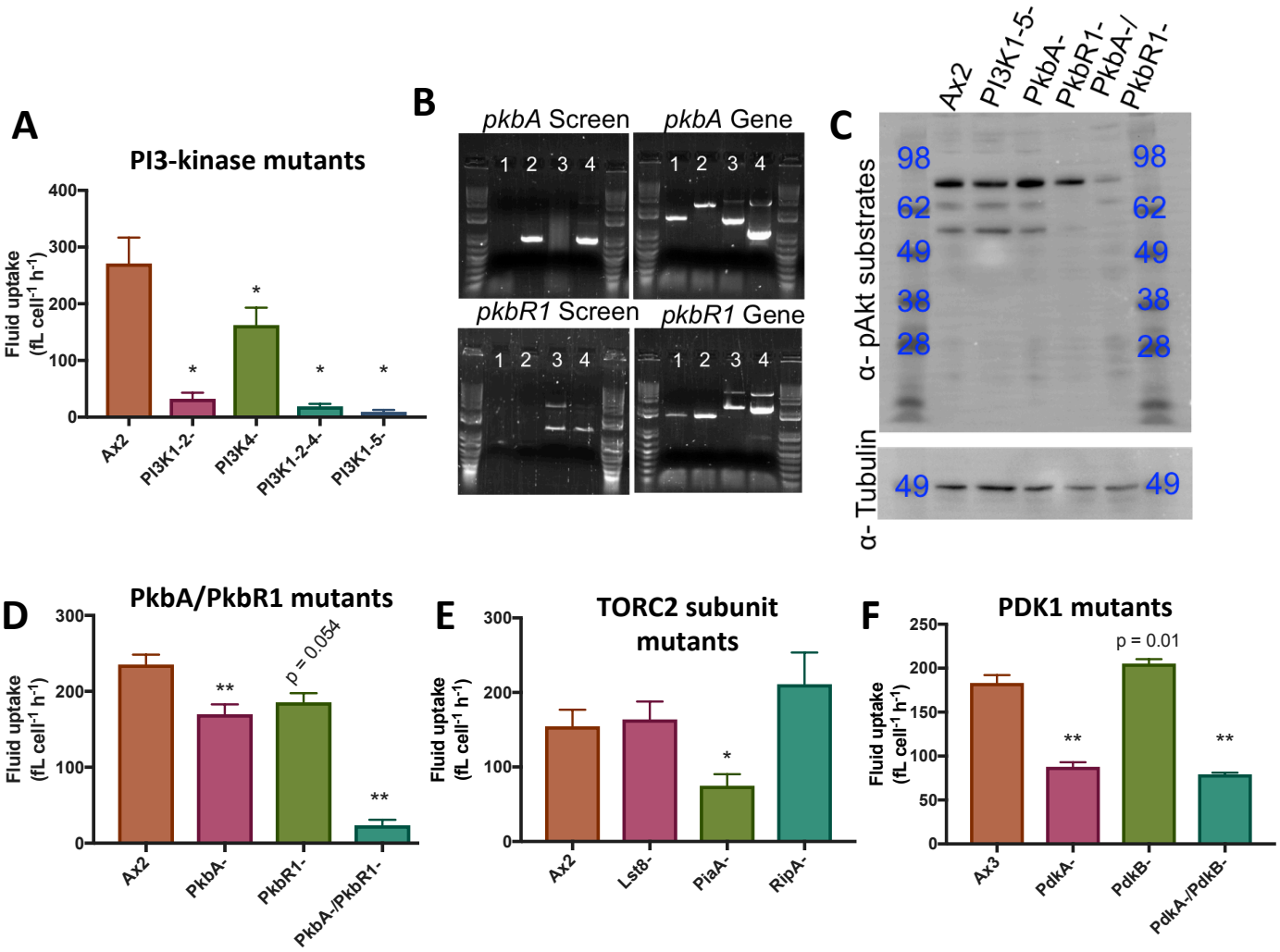

Figure S1; related to figure 1: Isolation and characterisation of PkbA/PkbR1 mutants and upstream activators

A) PI3-kinase mutants had similar fluid uptake defects after 24 h incubation in HL5 medium + 10% FBS compared to HL5 alone (Figure 1A). **B)** PCRs confirming the knockout of PkbA and PkbR1. The "gene" PCRs go across the full length of the gene, and are altered in length in the mutants while the "screen" PCRs are only visible in the mutants. Ax2 is shown in lane 1, PkbA- in lane 2, PkbR1- in lane 3 and PkbA-/PkbR1- in lane 4. Genomic DNA was prepared using a Zymogen gDNA miniprep kit according to the manufacturers instructions. **C)** PkbA-/PkbR1- mutants have negligible Akt substrate phosphorylations, while PI3K1-5- and single mutants are largely unaffected at a global level. **D)** Fluid uptake of PkbA/PkbR1 mutants was measured by TRITC-dextran addition for 1 h after 24 h incubation in HL5 medium + 10% FBS following harvesting from bacteria for PkbA/PkbR1 mutants, with similar fluid uptake defects observed as when they were incubated in HL5 alone (Figure 1B). Fluid uptake was generally improved, compared to HL5 medium alone (Figures 1C&1E) by addition of 10% FBS for **E)** TORC2 subunit mutants and **F)** PDK1 mutants.

For fluid uptake determination, cells were harvested from bacteria and inoculated in HL5 medium + 10% FBS for 24 h, after which TRITC-Dextran was added for 1 h. Cells were washed in ice-cold KK_2 buffer, detached and analysed by flow cytometry. Graphs show mean ± SEM, n = 3. $p \leq 0.1$ is specified, * $p < 0.05$, ** $p < 0.01$ compared to parent strain. For western blots, cells were incubated in HL5 medium + 10% FBS for 24 h before protein was harvested and lysate from approximately $2x10^5$ cells run out. The size of the protein markers are shown in kDa in blue text.

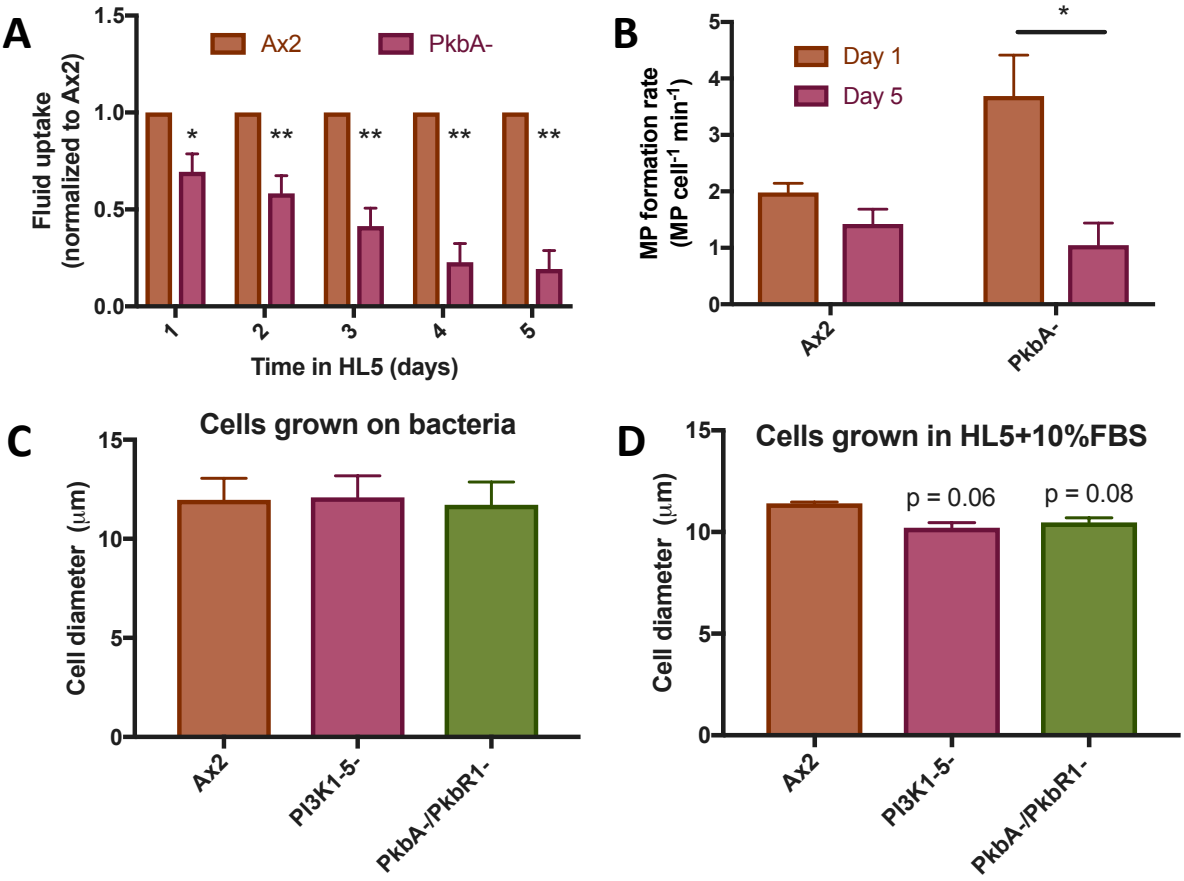

Figure S2; related to figure 2: PkbA- macropinocytosis over time and PkbA-/PkbR1- cell size
A) Fluid uptake decreases over time in PkbA- cells, accounting for the unexpected growth defect (Figure 2A). Ax2 and PkbA- cells were harvested from bacteria and inoculated into HL5 in 96-well plates at various densities, to account for cell proliferation, and fluid uptake measured every day for 5 days. **B)** The decrease in fluid uptake over time in PkbA- cells is due to a decrease in macropinosome formation. Ax2 and PkbA- cells were harvested from bacteria into HL5 for 1 or 5 days, after which their macropinosome formation rate was measured by pulsing cells for 1 min with FITC-dextran, fixing them and counting the number of macropinosomes by microscopy. **C)** PI3K1-5- and PkbA-/PkbR1- cells are the same size as Ax2 cells when cultivated on bacteria, where there is no proliferation defect (n = 4). Cells were grown on SM agar, washed and inoculated into KK_2MC + *Ka* bacteria for 24 h before being washed, resuspended in KK_2MC and size measured using an Eclipse (Sony iCyt) **D)** The PI3K1-5- and PkbA-/PkbR1- cell diameter is slightly decreased after they have been incubated in HL5 medium + 10% FBS for 24 h. Cells were prepared as in C.
Graphs show mean ± SEM, n = 3 unless stated, $p < 0.1$ is stated, * $p < 0.05$, ** $p < 0.01$ compared to Ax2.

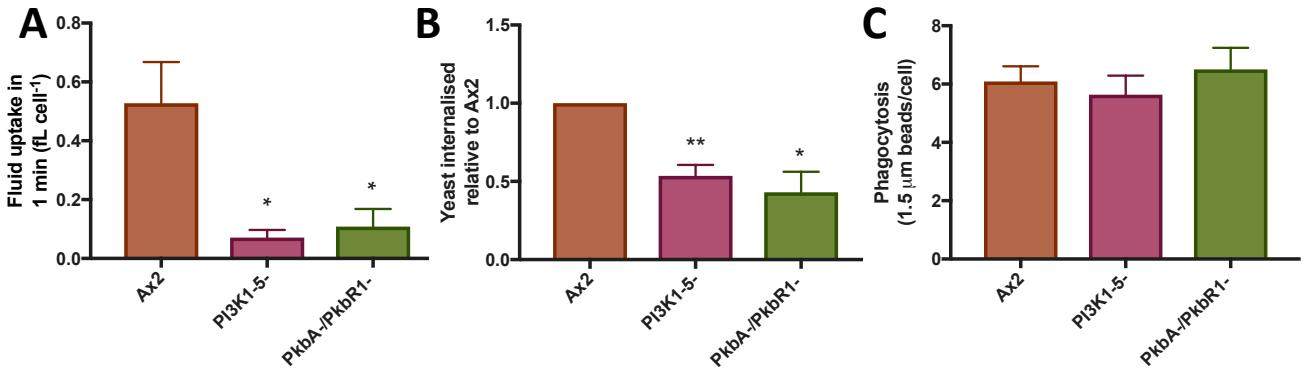

Figure S3; related to figure 4: PI3K1-5- and Akt- cells do not have increased endosome recycling, but do have reduced large particle uptake

A) The fluid uptake decrease observed in PI3K1-5- and PkbA-/PkbR1- cells is apparent after 1 min. Cells were harvested from bacteria and incubated in HL5 medium + 10% FBS for 24 h. The medium was then swapped to SUM for ≥1.5 h to minimise background fluorescence. Fluid uptake was then measured using 5 mg/ml TRITC-Dextran (n = 4). As this decrease is greater than for the macropinosome formation rate (Figure 4A), increased endosome recycling cannot account for the fluid uptake defects. **B)** Yeast endocytosis is reduced in PI3K1-5- and PkbA-/PkbR1- cells, consistent with these mutants having smaller macropinocytic patches (Figure 4C). Cells were harvested from bacterial SM agar plates, washed and incubated with fluorescent yeast for 1 h, after which the non-phagocytosed yeast fluorescence was quenched with trypan blue. Internalised fluorescence was measured on a fluorimeter and set relative to Ax2. **C)** Phagocytosis of 1.5 µm beads is unaffected in the PI3K1-5- and PkbA-/PkbR1- mutants, indicating there is no general phagocytosis defect in these cells. Cells were harvested as in B then distributed into 96-well plates in KK_2MC and allowed to settle. 1.5 µm beads were added to $1x10^8$ beads/ml for 20 min, after which the cells were washed, detached and analysed by flow cytometry.
Graphs show mean ± SEM, n = 3 unless otherwise stated, * $p < 0.05$, ** $p < 0.01$ compared to Ax2.

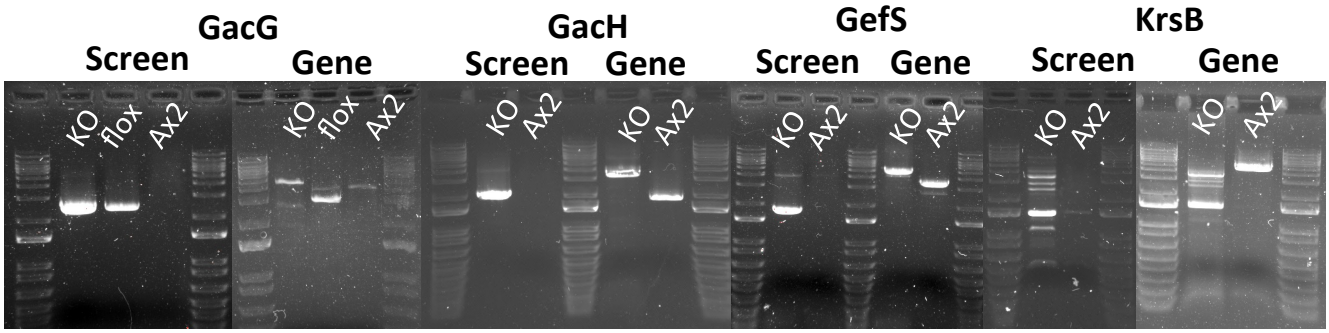

Figure S4; related to figure 5: Knockout of PkbA/PkbR1 targets

PCRs confirming the knockout of proteins identified in the phosphoproteomic screen. "Screen" PCRs only have a product when the gene is knocked out, while the "Gene" PCRs are across the full-length gene and have altered size in the mutants. Genomic DNA was prepared using a Zymogen gDNA miniprep kit according to the manufacturers instructions.

A

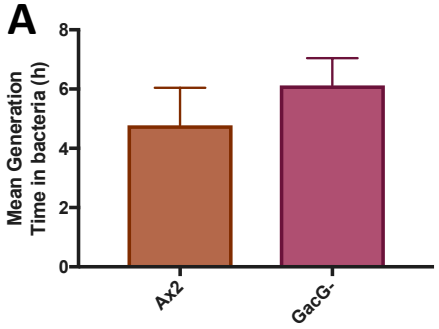

B

Strain	Macropinosome "diameter" (%)	Macropinosome radius (%)	Macropinosome volume (%)
Ax2	100 (1.30 µm)	100 (0.75 µm)	100 (1.78 µm^3)
GacG-	75	75	41

C

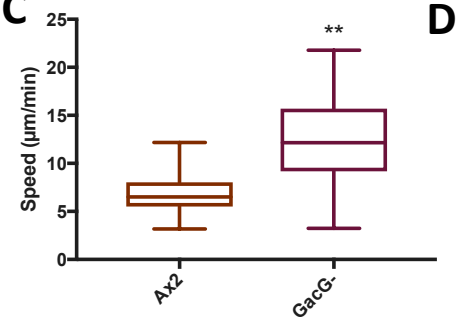

D

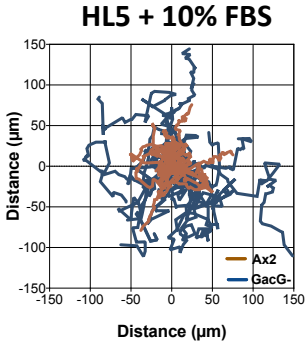

E

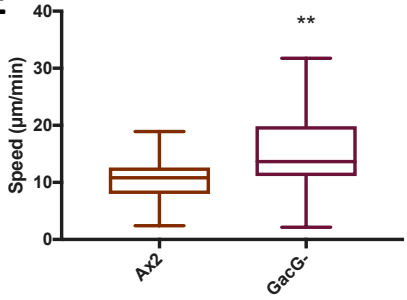

F

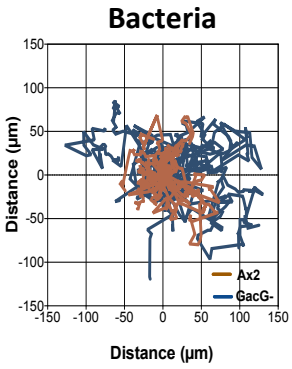

G

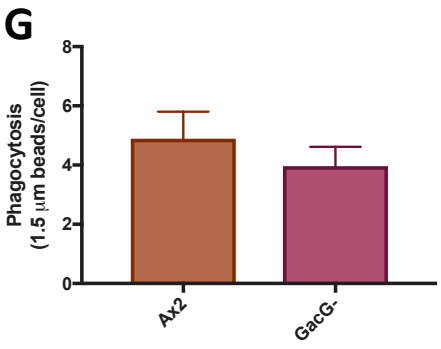

H

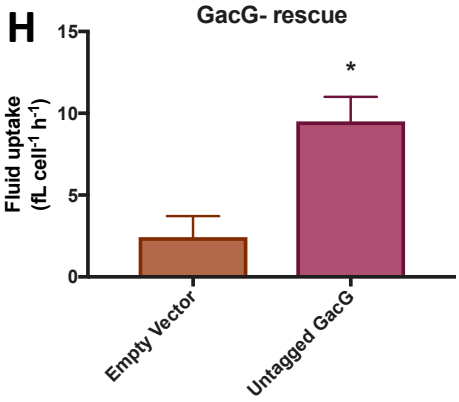

Figure S5; related to figure 6: GacG- cell proliferation, endocytosis and movement (previous page)
A) GacG- cells proliferate normally on bacteria. Cells were harvested from growth on SM bacterial plates and incubated in 20 $OD_{600\ nm}$ *Ka* in KK_2MC at 22 °C, 220 rpm. Cell density was determined at regular intervals using a hemacytometer. **B)** Summary table of Figure 6C showing the average values as a percentage of the parent control. The measured diameter of the macropinosomes tends to halfway between the equator and the poles of the macropinosome (assuming the observed diameters were obtained from random sections of perfectly spherical macropinosomes). The average radius is calculated by multiplying the median observed diameter by tan(30°), and the volume calculated from that. As macropinosomes are often not perfect spheres when they are formed, and sampling at the periphery of macropinosomes is technically challenging, these values are approximate. **C)** GacG- cells move faster than Ax2 cells when grown axenically in HL5 medium + 10% FBS. The speed of 120 randomly moving cells was measured over 20 minutes using a Zeiss 700 series microscope. **D)** The tracks of 20 cells incubated in HL5 medium + 10% FBS for 24 h, then filmed randomly moving using a Zeiss 700 series microscope from Figure 6G are shown. **E)** GacG- cells move faster than Ax2 cells when grown on bacteria. The speed of 120 randomly moving cells was measured over 20 minutes using a Zeiss 700 series microscope. **F)** The tracks of 20 cells from E are shown. **G)** Phagocytosis of 1.5 µm beads is unaffected in the GacG- mutant, like the PkbA-/ PkbR1- and PI3K1-5- mutants, indicating there is no general phagocytosis defect in these cells. Cells were harvested from SM plates, distributed into 96-well plates in KK_2MC and allowed to settle. 1.5 µm beads were added to $1x10^8$ beads/ml for 20 min, after which the cells were washed, detached and analysed by flow cytometry. **H)** The fluid uptake defect of GacG- cells can be rescued by overexpression of untagged GacG, albeit to far below the levels of Ax2. GacG- cells were transformed with an empty expression vector, or the vector containing GacG. Transformants were selected for on bacteria, then transferred to HL5 medium + 10% FBS and fluid uptake was assessed 24-72h after transfer.
Bar graphs show mean ± SEM, box plots show the minimum and maximum values, the box is the 25^{th} to 75^{th} percentile and the middle line shows the median. n = 3 unless specified. * $p < 0.05$, ** $p < 0.01$ compared to Ax2 or the control.

Table S1: Phosphopeptide abundance in Akt mutant cells

The phosphopeptides identified by TMT mass spectrometry and their abundance in PkbA/ PkbR1 mutants relative to Ax2. Strains were harvested from bacterial plates, washed free of bacteria and incubated in HL5 medium + 10% FBS for 24 h at 22 ^{o}C, 220 rpm at 1-2x10^{6} cells/ ml. Cells were then washed free of medium, resuspended in KK_2MC buffer and treated for 30 minutes with DMSO or 100 µM LY294002 before protein was harvested, TMT tagged, phosphopeptides purified and analysed by mass spectrometry. The abundance of each phosphopeptide in each condition was measured relative to Ax2. Condition 1- Ax2, condition 2- PkbA-, condition 3- PkbR1-, condition 4- PkbR1- + LY294002, condition 5- PkbA-/PkbR1-.

Click here to Download Table S1

Uniprot ID	Dictybase ID	Phosphosite(s)	Most likely kinase	Predicted function
P0CD60	FrmC	S306	PKA	Cytoplasm/membrane linker
P28178	PkbR1	T432 ; S449 ; T470	PKC ; GSK3 ; GSK3	Protein Kinase
Q00766	GlpV	T10 ; T13	Cdc2 ; PKC	Glycogen phosphorylase
Q54B11	DDB_G0293990	S230	PKA	Unknown
Q54DP0	DDB_G0292106	S212	PKA	Endosomal transport
Q54ET0	GrlE	T765 ; S770	PKC ; CKII	GPCR
Q54GL1	GDE1	S271	PKA	Phosphodiesterase
Q54H00	DDB_G0289807	S531	PKA	Protein/Lipid phosphatase
Q54HC8	DDB_G0289551	S123	DNAPK	Membrane protein
Q54IA6	DDB_G0288895	T395	PKG	Unknown
Q54LB8	Vps13A	S1685	PKA	Vacuolar sorting
Q54P47	NdrC	S12 ; S529	RSK ; GSK3	Protein Kinase
Q54QE5	DDB_G0283919	S465	GSK3	Protein Phosphatase
Q54QI2	DDB_G0283821	S750	PKA	Proten Kinase
Q54R82	MkkA	S488	CAM-II	Proten Kinase
Q54RZ3	DDB_G0282823	S694	RSK	Unknown
Q54SC3	DDB_G0282779	S495	PKC	Transmembrane protein
Q54SL6	GacQ	T272	Cdc2	RhoGAP
Q54U31	ShkD	S267	PKA	Protein Kinase
Q54VX2	GxcS	S317	RSK	RhoGEF
Q54WH7	DDB_G0279653	S60	PKA	Unknown
Q552C1	DDB_G0276181	S268	PKA	Protein Kinase
Q553Q6	DDB_G0275401	S513	DNAPK	Unknown
Q555M9	DDB_G0274847	S989	Cdc2	Nucleotidyltransferase
Q55DM1	LvsA	S93	PKA	Contractile Vacuole protein
Q6XHA6	Roco10	S1671	Cdc2	LRRK family protein kinase
Q86C65	Tor	S454	PKA	Protein Kinase
Q86KF9	SgkA	S424	Cdc2	Sphingosine Kinase
Q54TT8	DDB_G0281503	S938	PKA	Unknown

Table S2: Candidate proteins involved in macropinocytosis not phosphorylated by PkbA/PkbR1
Phosphorylated proteins that were less abundant in PkbA/PkbR1 mutants (>4-fold decreased in PkbA-/PkbR1- cells, >2-fold in PkbR1- + LY294002) compared to Ax2 which did not have an Akt consensus motif. Cells were incubated for 24 h in HL5 medium + 10% FBS at 22 ^{o}C, 220 rpm to allow macropinocytosis upregulation, then washed and resuspended in KK_2MC and treated with 100 µM LY294002 inhibitor or DMSO for 30 min. Proteins were then precipitated, labelled with TMT tags, enriched for phosphopeptides and the abundance of each compared using mass spectrometry.

GO molecular function term	Proteins matching terms (Total proteome)	Proteins matching terms (Akt targets)	Expected proteins	Fold Enrichment	Raw P-value	False Discovery Rate
clathrin light chain binding (GO:0032051)	2	1	0	> 100	0.0035	1.56
clathrin adaptor activity (GO:0035615)	2	1	0	> 100	0.0035	1.30
endocytic adaptor activity (GO:0098748)	2	1	0	> 100	0.0035	1.12
phosphatidylinositol-3,4-bisphosphate binding (GO:0043325)	3	1	0	> 100	0.0047	1.30
phosphatidylinositol-3,5-bisphosphate binding (GO:0080025)	3	1	0	> 100	0.0047	1.16
cargo receptor activity (GO:0038024)	4	1	0	> 100	0.0059	1.30
protein-containing complex scaffold activity (GO:0032947)	8	1	0.01	> 100	0.0105	1.46
clathrin binding (GO:0030276)	10	1	0.01	84.9	0.0129	1.68
molecular adaptor activity (GO:0060090)	14	1	0.02	60.64	0.0175	1.76
protein binding, bridging (GO:0030674)	14	1	0.02	60.64	0.0175	1.69
Rac GTPase binding (GO:0048365)	15	1	0.02	56.6	0.0187	1.66
phosphatidylinositol bisphosphate binding (GO:1902936)	15	1	0.02	56.6	0.0187	1.59
microtubule motor activity (GO:0003777)	17	1	0.02	49.94	0.0210	1.72
phosphatidylinositol phosphate binding (GO: 1901981)	31	1	0.04	27.39	0.0370	1.91
Rho GTPase binding (GO:0017048)	68	2	0.08	24.97	0.0030	1.65
motor activity (GO:0003774)	34	1	0.04	24.97	0.0404	1.99
microtubule binding (GO:0008017)	44	1	0.05	19.3	0.0517	2.44
Rho guanyl-nucleotide exchange factor activity (GO:0005089)	46	1	0.05	18.46	0.0539	2.39
tubulin binding (GO:0015631)	53	1	0.06	16.02	0.0617	2.68
phosphatidylinositol binding (GO:0035091)	54	1	0.06	15.72	0.0628	2.68
guanyl-nucleotide exchange factor activity (GO:0005085)	114	2	0.13	14.89	0.0080	1.47
GTPase activator activity (GO:0005096)	116	2	0.14	14.64	0.0082	1.41
GTPase regulator activity (GO:0030695)	117	2	0.14	14.51	0.0084	1.33
nucleoside-triphosphatase regulator activity (GO:0060589)	124	2	0.15	13.69	0.0094	1.38
Ras guanyl-nucleotide exchange factor activity (GO:0005088)	64	1	0.08	13.27	0.0738	2.92
GTPase binding (GO:0051020)	195	3	0.23	13.06	0.0015	1.08
phospholipid binding (GO:0005543)	74	1	0.09	11.47	0.0847	3.13
Ras GTPase binding (GO:0017016)	149	2	0.18	11.4	0.0132	1.63
small GTPase binding (GO:0031267)	149	2	0.18	11.4	0.0132	1.54
phosphoprotein phosphatase activity (GO: 0004721)	76	1	0.09	11.17	0.0869	3.11
enzyme activator activity (GO:0008047)	155	2	0.18	10.95	0.0142	1.58
molecular function regulator (GO:0098772)	326	4	0.38	10.42	0.0005	1.06

Table S3; related to table 1 and figure 5: Terms enriched by GO analysis in the Akt target proteins
The 16 proteins identified as being phosphorylated at an Akt consensus sequence with a reduced abundance by mass spectrometry (Table 1) were subject to GO analysis against the *Dictyostelium discoideum* proteome. The terms with a >10-fold enrichment are shown here. Statistical analysis was performed using fishers exact test.

	Uniprot ID	Dictybase ID	Phosphosite(s)	Most likely kinase	Predicted function
PkbA dependent	Q55FS2	KrsB	S505	Akt	Protein Kinase
	Q6S004	Kif6	S1016	Akt	Kinesin
PkbR1 dependent	Q54YK2	DDB_G0278629	S679	Akt	Unknown
	Q8SSW7	GefS	S623	Akt	RasGEF

Table S4 related to table 1 and figure S4: PkbA and PkbR1 dependent phosphorylations
The proteins with phospho-sites which appear to be dependent on either PkbA or PkbR1 specifically. Phosphopeptides that had an Akt recognition motif were identified which were >4-fold reduced compared to the Ax2 control in either PkbA- cells (PkbA-dependent phosphorylations) or PkbR1- cells (PkbR1-dependent phosphorylations).

Parent	Mutation(s)	Resistance	Strain reference(s)	Source
Ax2 (Ka)	-	-	Ax2 (Ka)	Rob Kay
Ax2 (Ka)	*pi3k1-/2-*	Blasticidin	HM1141	(Hoeller and Kay, 2007)
Ax2 (Ka)	*pi3k4-*	Blasticidin	HM1148	(Hoeller and Kay, 2007)
Ax2 (Ka)	*pi3k1-/2-/4-*	Blasticidin	HM1159	(Hoeller and Kay, 2007)
Ax2 (Ka)	*pi3k1-5-*	Blasticidin	HM1200	(Hoeller and Kay, 2007)
Ax2 (Ka)	*pkbA-*	G418	HM1815-7	This work
Ax2 (Ka)	*pkbA-*	-	HM1818	This work
Ax2 (Ka)	*pkbR1-*	G418	HM1832-4	This work
Ax2 (Ka)	*pkbR1-*	-	HM1835	This work
Ax2 (Ka)	*pkbA-/pkbR1-*	G418	HM1850-2	This work
Ax2 (Ka)	*pkbA-/pkbR1-*	-	HM1853	This work
Ax2 (Ka)	*lst8-*	Blasticidin	HM1415	Louise Fets
Ax2 (Ka)	*piaA-*	Blasticidin	HM1461	Louise Fets
Ax2 (Ka)	*ripA-*	Blasticidin	HM1364	Oliver Hoeller
Ax3 (Devreotes)	-	-	Ax3 (Devreotes)	Peter Devreotes
Ax3 (Devreotes)	*pdkA-*	Blasticidin	HM1950	(Kamimura and Devreotes, 2010)
Ax3 (Devreotes)	*pdkB-*	Blasticidin	HM1951	(Kamimura and Devreotes, 2010)
Ax3 (Devreotes)	*pdkA-/B-*	Blasticidin	HM1952	(Kamimura and Devreotes, 2010)
Ax2 (Ka)	*gacG-*	G418	HM1945-9	This work
Ax2 (Ka)	*gacG-*	-	HM1956	This work
Ax2 (Ka)	*gacH-*	G418	HM1942-4	This work
Ax2 (Ka)	*krsB-*	G418	HM1970-3	This work
Ax2 (Ka)	*gefS-*	G418	HM1953-5	This work
Ax4 (Kuspa)	-	-	Ax4 (Kuspa)	Adam Kuspa
Ax4 (Kuspa)	*scaA-*	Blasticidin	V10285	(Sawai et al., 2008)

Table S5: Strains used in this study
The strains used in this study. Where there is more than one strain of a particular mutant, the phenotype presented in the text is representative of all the strains. Where strains have been cured of their resistance by cre-lox recombination, the data represented in this work is of the strain without a resistance cassette.

Hoeller, O. and Kay, R. R. (2007). Chemotaxis in the absence of PIP3 gradients. *Curr. Biol.* **17**, 813-817.
Kamimura, Y. and Devreotes, P. N. (2010). Phosphoinositide-dependent protein kinase (PDK) activity regulates phosphatidylinositol 3,4,5-trisphosphate-dependent and -independent protein kinase B activation and chemotaxis. *J. Biol. Chem.* **285**, 7938-46.
Sawai, S., Guan, X. J., Kuspa, A. and Cox, E. C. (2008). High-throughput analysis of spatio-temporal dynamics in *Dictyostelium*. *Genome Biol.* **8**, R144 (15 pages).

Vector	Markers	Selection
pDM1140	PakB CRIB-GFP (active Rac), Raf1 RBD-mCherry (active Ras)	G418
pDM1383	HSPC300-GFP (SCAR), Raf1 RBD-mCherry (active Ras)	G418
pDM1489	Cre Recombinase	Hygromycin
pPI157	Raf1 RBD-GFP (active Ras)	G418
pPI321	Raf1 RBD-GFP (active Ras), Lifeact-mCherry (F-actin)	G418
pTW001	Raf1 RBD-GFP (active Ras), PTEN-mCherry	G418
pTW002	Raf1 RBD-GFP(active Ras), PH PkgE-mCherry (PIP3)	G418
pDM1207	Empty Vector control	G418
pTW003	GFP-PkbA	G418
pTW044	GFP-PkbA T435A	G418
pTW046	GFP-PkbA T278A	G418
pDM1209	Empty Vector control	G418
pTW008	PkbR1-GFP	G418
pTW063	PkbR1-GFP T470A	G418
pTW065	PkbR1-GFP T309A	G418
pTW032	GacG-GFP	G418
pPI582	GFP-GacG	G418
pDM1203	Empty Vector control	G418
pTW058	GacG	G418

Table S6: Over-expression vectors used in this study
The overexpression vectors used in this study. These were made based in the pDM expression system (Veltman et al., 2009).

Veltman, D. M., Akar, G., Bosgraaf, L. and Van Haastert, P. J. (2009). A new set of small, extrachromosomal expression vectors for *Dictyostelium discoideum*. *Plasmid* **61**, 110-118.

Vector name	Target gene	Linearising digest	Selection marker	Construction details
pPkbAKO	*pkbA*	SmaI	G418	G418, 5' and 3' KO arms amplified and then joined by PCR. Product was cloned into pJet1.2 (Thermo-Fisher)
pPkbR1KO	*pkbR1*	SmaI	G418	G418, 5' and 3' KO arms amplified and then joined by PCR. Product was cloned into pJet1.2 (Thermo-Fisher)
pGacGKO	*gacG*	BamHI & SpeI	G418	Gene amplified from Ax2 DNA and cloned into pJet1.2 (Thermo-Fisher). Digested with EcoRV and a G418 EcoRV digest inserted.
pGacHKO	*gacH*	BamHI & NheI (partial digest)	G418	Gene amplified from Ax2 DNA and cloned into pJet1.2 (Thermo-Fisher). Digested with EcoRV and a G418 EcoRV digest inserted.
pGefSKO	*gefS*	BglII/SpeI	G418	Gene amplified from Ax2 DNA and cloned into pJet1.2 (Thermo-Fisher). Digested with EcoRV and a G418 EcoRV digest inserted.
pKrsBKO	*krsB*	PvuI	G418	Gene amplified from Ax2 DNA and cloned into pJet1.2 (Thermo-Fisher). Digested with EcoRV and a G418 EcoRV digest inserted.

Table S7: Knockout vectors used in this study
The knockout vectors used in this study and how they were made. The resistance cassette was obtained from pDM vectors.

Table S8: Primers used in this study (overleaf)
The primers used in this study, and what they were used to amplify. Restriction enzyme sites incorporated into the sequences are shown in lower case, while overlapping primer sequences are shown in lower case and italicised. Introduced point mutations are shown in bold.

PCR product	Primer 1 name	Primer 2 name	Primer 1 sequence	Primer 2 sequence
pkbA gene	pkbA_F	pkbA_R	agatctATGTCAACAGCACCAATTAAA	actagtTTATCTTAAATGTTCAGATTC
pkbR1 gene	pkbR1_F	pkbR1_R	agatctATGGGAAAAGGACAAAGTAAA	actagtATCCTTTAAGATTGAATCAGC
gacG gene	gacG_F	gacG_R	ggatccATGGCGTCAATATTTTTAAATAAAAAAC	actagtCTCTTCAACAATATCAGTTAAAGAAGG
gacH gene	gacH_F	gacH_R	agatctATGAGTGGTGTAGGAGGTGAATCAGTAC	gctagcATTATCATAAAATAAATTATAATTTTCAATTAATAAAG
krsB gene	krsB_F	krsB_R	ggatccATGGAGGAAAGTGGTCAAC	aagctagcATTATTATAAAAATCTAAATCAAATTCTGAATAAAT
gefS gene	gefS_F	gefS_R	agatctATGGGAGAAGTAAGTTTAATCGG	actagtCTTTGGTTCGAGAGCAATTGATA
pDM resistance cassette	oDM1015	oDM1016	CTTCAGTAGGCAGAGCTATC	CAGCTTGGATACTCCAGTAG
pkbA KO 5' arm	pkbA_5'F	pkbA_5'R	cccgggCCAAACCACAACAATATTCGCATAA	*gatagctctgcctactgaag*TCCATTAACTCTTTTCTTACGATCAGA
pkbA KO 3' arm	pkbA_3'F	pkbA_3'R	*ctactggagtatccaagctg*TTGACACCAACCGACAAAACTG	cccgggTCTTAAATGTTCAGATTCAGCGACA
pkbR1 KO 5' arm	pkbR1_5'F	pkbR1_5'R	cccgggTTTAATTACCACACTGTCACTATTTCCTATAAG	*gatagctctgcctactgaag*TTGATAAAAGACTTGGAACTAAAG
pkbR1 KO 3' arm	pkbR1_3'F	pkbR1_3'R	*ctactggagtatccaagctg*GTCCTTCATCTTCATCATCATT	cccgggACTCTCTTTCTCACACCAATAACAC
pkbA screen	pkbA_ExtR	oDM1014	TTTTACCAAAGACGGAAACTTATTCTAAC	CTACTGGAGTATCCAAGCTG
pkbR1 screen	pkbR1_ExtR	oDM1014	cccgggCACAAACCAAATAAAAGTATTCATCATGTC	CTACTGGAGTATCCAAGCTG
gacG screen	gacG_5F4	oPI236	ATTACACATATATACATAAAATATTCAAAACCACAC	atctcgAGAGTAGTATAACTTCGTATAGCATAC
gacH screen	gacH_5F1	oPI236	TTAAAAGAGGGTGTTAATTGAAATTTC	atctcgAGAGTAGTATAACTTCGTATAGCATAC
krsB screen	krsB_Ext3'	oPI236	GGTAATTTCCTCTTTTGAAGCCATT	atctcgAGAGTAGTATAACTTCGTATAGCATAC
gefS screen	gefS_Ext5'	oPI236	TTTAAATATACTTCACTCTCTCCCAAGT	atctcgAGAGTAGTATAACTTCGTATAGCATAC
pkbA T278A point mutation	pkbA_T278A_F	pkbA_T278_R	**GCT**TTCTGTGGTACTCCTGAATATTTAGC	ACCAGTTTTGTCGGTTGGTGTCAATAGACCCTC
pkbA T435A point mutation	pkbA_T435A_F	pkbA_T435_R	**GCA**TATGTCGCTGAATCTGAACATTTAAG	AAATCCTTCAAAATCTTTTTGTTGTTGCGG
pkbR1 T309A point mutation	pkbA_T309A_F	pkbA_T309_R	**GCT**TTCTGTGGTACACCAGAGTATTTAGC	GAATGTACCATCGGTTGTTTCAAT
pkbR1 T470A point mutation	pkbA_T470A_F	pkbA_T470_R	**GCT**TATGTAGCTGATTCAATCTTAAAGG	GAAACCTTCAAAGCTTGTATC